Facies (2023) 69:9
https://doi.org/10.1007/s10347-023-00663-w

ORIGINAL ARTICLE

Revisiting the upper Visean mud mounds from Derbyshire (UK): the role of brachiopods in their growth

Alessandro P. Carniti[1] · Giovanna Della Porta[1] · Vanessa J. Banks[2] · Michael H. Stephenson[2,3] · Lucia Angiolini[1]

Received: 12 October 2022 / Accepted: 14 March 2023 / Published online: 25 April 2023

Abstract

Several brachiopod-rich mud mounds occur in the upper Visean (Brigantian) of the Derbyshire Carbonate Platform succession in UK. The re-evaluation of the lithofacies architecture of a Derbyshire mud mound complex, developed in an intraplatform middle-ramp environment, led to the recognition of three lithofacies associations: (a) a 10 m thick basal unit of automicrite boundstone with siliceous sponge spicules and brachiopod–bryozoan packstone to wackestone beds; (b) a 10 m thick, 250 m wide, lens-shaped, convex-up massive core of clotted peloidal micrite and fenestellid bryozoan boundstone with sponge spicules; (c) inclined brachiopod–bryozoan–crinoid packstone flank beds. In the mud mound complex core, most of the carbonate mud with clotted peloidal and structureless micrite fabric is the result of biologically induced and influenced in-situ precipitation processes (automicrite). Brachiopods are not, as previously thought, limited to storm-scoured "pockets" in the mud mound complex core but are abundant and diverse in all lithofacies and lived on the irregular mud mound complex surface concentrating in depressions sustained by automicrite boundstone and the growth of bryozoans and sponges. The upper Visean Derbyshire mud mounds are, thus, representatives of a newly defined fenestellid bryozoan–brachiopod–siliceous sponge mud mound category, occurring in various middle–upper Visean Western European sites, a sub-type of the fenestellid bryozoan–crinoid–brachiopod Type 3 buildups of Bridges et al. (1995). These mud mounds, and other types of brachiopod-rich buildups, developed in carbonate platform settings between fair-weather and storm wave base, in dysphotic environments with dispersed food resources during the Visean. Brachiopod mud mound colonisation was favoured by moderate water depth, availability of food resources, and diverse substrates.

Keywords Mississippian · Visean · Mud mound · Reef · Brachiopod · Derbyshire

Introduction

The sedimentary record of Mississippian carbonate depositional systems is characterised by the abundance of mud mounds, i.e. lenticular buildups with a substantial proportion of carbonate mud (> 30%, Bridges et al. 1995; > 50%, Reitner and Neuweiler 1995) associated with metazoan skeletal components not forming a skeletal framework (bryozoans, sponges, crinoids, brachiopods, calcareous algae; sensu Wilson 1974, Bosence and Bridges 1995, Monty 1995, Pratt 1995, Bridges et al. 1995, Reitner and Neuweiler 1995). In mud mounds, carbonate mud is largely precipitated in situ through biologically induced and influenced processes (e.g. Lees and Miller 1985, 1995; Monty 1995; Pickard 1996). According to the broad reef definitions proposed by Riding (2002) and Flügel and Kiessling (2002), mud mounds are a category of reefs, representing "laterally confined biogenic structures, developed by the growth or activity of sessile benthic organisms and exhibiting topographic relief and (inferred) rigidity" (Flügel and Kiessling 2002, p. 3). Terms such as "bioconstruction", "bioherm", and "buildup" are synonymous with reef (Flügel and Kiessling 2002). The term "reef mound" (James 1978, 1983) indicates mud mounds with a high density of bioclastic material and

✉ Alessandro P. Carniti
alessandro.carniti@unimi.it

[1] Dipartimento Di Scienze Della Terra "A. Desio", Università Degli Studi Di Milano, Via Mangiagalli 34, 20133 Milan, Italy

[2] British Geological Survey, Nicker Hill, Keyworth NG12 5GG, Nottinghamshire, UK

[3] Stephenson Geoscience Consulting Ltd, Keyworth, Nottingham, UK

few automicrites, while "microbial mound/reef" (James and Bourque 1992; Chevalier and Aretz 2005) is used for mud mounds built by calcimicrobe crusts, stromatolite, thrombolite, and other microbial precipitates.

The microbial–metazoan community responsible for the growth of mud mounds was increasingly common from the late Frasnian (Webb 1996, 2002) and became widespread after the extinction of metazoan reef frame-builders (e.g. stromatoporoids, rugose and tabulate corals) at the Frasnian–Famennian boundary (Kellwasser Extinction Event; e.g. Wright and Faulkner 1990; Buggisch 1991) and at the end of the Devonian (Hangenberg Event; e.g. Yao et al. 2016, 2020).

Carbonate mud precipitation associated with microbial mats and other organic substrates in marine and non-marine present-day and ancient settings can take place through different pathways: (a) mediated by the metabolic activity of microbial communities (biologically induced mineralisation sensu Dupraz et al. 2009), or (b) result from the interaction of $CaCO_3$-supersaturated water with organic substrates (biologically influenced mineralisation sensu Dupraz et al. 2009), e.g. decaying organic tissues such as biofilm extracellular polymeric substances (EPS) in microbial mats or siliceous sponges (organomineralisation sensu Trichet and Défarge 1995, Reitner et al. 1995a, 1995b). These processes produce characteristic textures in the carbonate mud precipitates: sub-millimetric peloids with diffuse margins, commonly surrounded by a microsparite mosaic, defined as clotted peloidal micrite (Pickard 1996), or structureless micrite, gravity-defying, sustaining millimetre-size primary cavities, termed leiolite (Braga et al. 1995). In Mississippian mud mounds, most carbonate mud is interpreted as precipitated through microbially mediated in situ processes (Lees and Miller 1995; Monty 1995; Pickard 1996) and/or passive organomineralisation of sponge soft tissues (Reitner et al. 1995a, b), based on the presence of such textures in the carbonate mud (Pickard 1996). Collectively, in situ carbonate mud precipitates related to processes of biologically induced and influenced mineralisation are referred to as "automicrite" (Wolf 1965; Reitner et al. 1995a). Mud-grade carbonate sediment, either produced by carbonate grain abrasion and bioerosion, or by reworking of in situ precipitates, was also common in some mud mounds, and labelled as allomicrite (Wolf 1965; Lees and Miller 1985; Devuyst and Lees 2001).

Mississippian mud mounds varied in size, carbonate mud textures, and skeletal assemblages. Some classification schemes have been proposed, mainly based on the skeletal assemblage, by Lees et al. (1985), Lees and Miller (1985, 1995), Bridges et al. (1995), and Somerville (2003).

Upper Tournaisian Waulsortian mud mounds, characterised by fenestellid bryozoans and siliceous sponge spicules in the core (Lees 1988; Lees and Miller 1995; Type 1 buildups in the classification of Bridges et al. 1995 and Somerville 2003), developed in outer-ramp settings, i.e. below storm wave base (sensu Burchette and Wright 1992), and mainly crop out in present-day Belgium (e.g. Lees et al. 1985), Ireland (e.g. Lees 1964; Sevastopulo 1982; Somerville et al. 1992), England (e.g. Miller and Grayson 1972; Bridges and Chapman 1988), and USA (e.g. Pray 1958; Cotter 1965; Precht and Shepard 1989).

These mud mounds consist of complexes resulting from the accretion of individual mounds (sensu Gutteridge 1995; Aretz and Chevalier 2007), up to 400 m in thickness and some kilometres in width (Lees and Miller 1995; Somerville 2003). Waulsortian mud mounds show skeletal assemblages varying vertically in the complexes. Lees et al. (1985) and Lees and Miller (1985, 1995) proposed a bathymetric succession of four "Waulsortian phases" based on the skeletal assemblages, from deeper to shallower (phases A–D). Also, Waulsortian mud mounds are characterised by multicomponent muds ("polymuds"; Lees and Miller 1985, 1995; Devuyst and Lees 2001), highly structured mud deposits showing successive geopetal fillings of different mud generations in primary cavities.

Other mud mound types developed in middle to outer-ramp settings in the Mississippian include crinoid–fenestellid bryozoan mud mounds with green shale in the core in the Tournaisian of Kentucky (Ausich and Meyer 1990; Meyer et al. 1995; Type 2 buildups in the classification of Bridges et al. 1995), and skeletal-rich mud mounds with a diverse bryozoan community, dasycladacean algae, and rugose corals in the Visean of northwest Ireland (e.g. Schwarzacher 1961; Kelly and Somerville 1992) and Algeria (Madi et al. 1996; Waulsortian-type or Type 1A mounds in the classification scheme of Somerville 2003). Trepostome bryozoan–microthrombolite mud mounds commonly with serpulid and problematic worm tubes (Type 5 buildups of Bridges et al. 1995) occurring in the Maritime Provinces of Canada (e.g. Dix and James 1989; Boehner 1989; Boehner et al. 1989), developed in lower–upper Visean deep basinal to shallow-water high-energy hydrothermal-seep-related settings (von Bitter et al. 1990, 1992; Boehner et al. 1989; Webb 2002).

Also in the Visean, crinoid–brachiopod–fenestellid bryozoan mud mounds (Type 3 buildups of Bridges et al. 1995), developed in platform interior, platform margin, inner- to middle-ramp, and intraplatform basin settings in Scotland (Pickard 1992) and Derbyshire in UK (Gutteridge 1995).

Finally, a wide spectrum of reefs built by calcimicrobe crusts (e.g. *Renalcis*, *Aphralysia*), corals, and lithistid sponges associated with automicrite and calcareous algae developed in Visean shallow, euphotic, high-energy shelf environments: e.g. coral–calcimicrobe reefs of northern England (Adams 1984; Horbury 1992), bryozoan–coral reefs in North Wales (Bancroft et al. 1988), microbial–sponge–bryozoan–coral reef in the upper Visean of Yorkshire, England

(Mundy 1994), and calcimicrobe–coral–sponge reefs in Queensland, Australia (Shen and Webb 2005, 2008), all of which were classified as Type 2 mounds by Somerville (2003) and as Type 4 buildups by Bridges et al. (1995), who did not consider them as mud mounds.

Despite the interest in characterising the skeletal composition of Mississippian buildups, most authors have neglected the important role of brachiopods, one of the prevailing benthic taxa in late Palaeozoic seas (Payne et al. 2014; Angiolini et al. 2021). In fact, several examples of Mississippian buildups have an abundant and diverse brachiopod fauna (e.g. Gutteridge 1995; Aretz and Chevalier 2007; Mottequin and Poty 2022). Brachiopod diversity and distribution are sensitive to environmental parameters such as substrate and food resources (e.g. Harper and Jeffrey 1996; Pérez-Huerta and Sheldon 2006; Angiolini 2007); hence, in brachiopod-rich mud mounds the combined study of lithofacies types and brachiopod communities provides fundamental information for the understanding of mud mound growth, depositional environment, water depth, and nutrient levels.

The aim of this study is the reassessment of the depositional lithofacies and brachiopod fauna distribution in brachiopod-rich mud mounds from the upper Visean of the Derbyshire Carbonate Platform, UK (Gutteridge 1990, 1995), according to Gutteridge (1990) brachiopods in the Derbyshire mud mounds are restricted to "storm-scoured" pockets in the mud mound surface. The final aim is to reach a better understanding of the palaeoenvironment and depositional model of the Derbyshire mud mounds. The studied mud mound complex in the Ricklow Quarry, Monyash, is compared with other brachiopod-rich Mississippian buildups, enhancing the knowledge on the variability of reefs after the end-Frasnian and end-Devonian extinctions.

Geological setting

During Tournaisian–Visean times central England, north of the Wales-Brabant High, was subdivided into basins and ranges due to north–south extensional tectonics (e.g. Leeder 1976, 1982; Gawthorpe et al. 1989; Guion et al. 2000; Stone et al. 2010).

One of the ranges was the Derbyshire High, between the Edale Basin to the north and the Widmerpool Gulf to the south (Fig. 1). The Derbyshire High is interpreted as comprising two basement tilted blocks, the Eyam Block to the north and the Woo Dale Block to the south (Smith et al. 1985), with a fault terrace in-between bounded by the Bakewell Fault and the Cronkston–Bonsall Fault (Fig. 2a; Gutteridge 1989a).

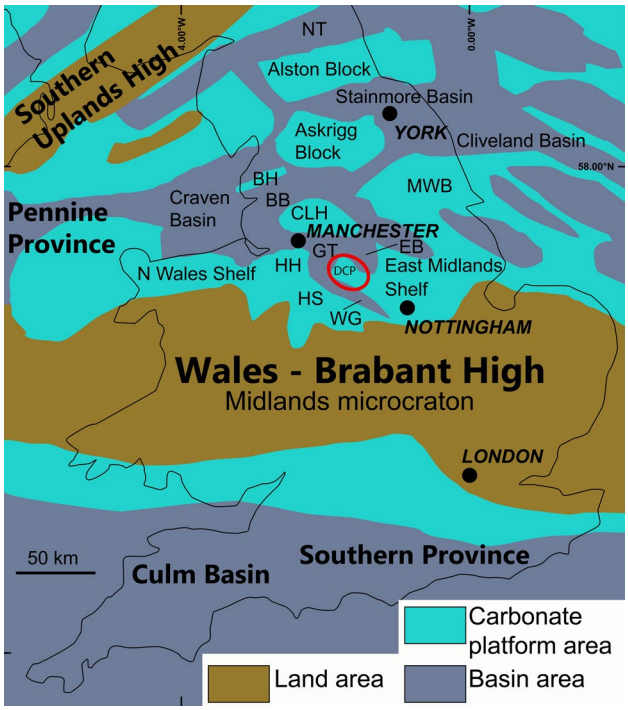

Fig. 1 Palaeogeographic context of the deposition of the Mississippian carbonate platforms of UK (Carboniferous Limestone Supergroup). The red ellipse indicates the southern Peak District, the outcrop area of the Derbyshire Carbonate Platform (DCP) on the Derbyshire High. *BB* Bowland Basin, *BH* Bowland High, *CLH* Central Lancashire High, *EB* Edale Basin, *GT* Gainsborough Through, *HH* Holme High, *HS* Hathern Shelf, *MWB* Market Weighton Block, *NT* Northumberland Trough, *WG* Widmerpool Gulf/Basin. Modified after Guion et al. (2000) and Waters et al. (2009)

In the late Tournaisian, the marine transgression on the Derbyshire High (Waters et al. 2009), situated at that time at subtropical latitudes (Piper et al. 1991; Woods and Lee 2018), led to the initiation of carbonate deposition on the irregular basement substrate: Woo Dale Limestone Formation (Fig. 2b; Aitkenhead and Chisholm 1982). In the late Visean, the area evolved into a flat-topped carbonate platform, characterised by peritidal deposition at estimated water depths of 0–25 m (Bridges 1982; Walkden 1987; Manifold et al. 2020), with skeletal grainstone shoals on the margins and sponge-microbial reefs at the break-in-slope to the north and west (Wolfenden 1958; Stevenson and Gaunt 1971; Broadhurst and Simpson 1973; Harwood 2005; Manifold et al. 2021): Bee Low Limestone Formation (Fig. 2b; Aitkenhead and Chisholm 1982).

Reactivation of extensional tectonics in the latest Visean, during deposition of the Monsal Dale Limestone Formation (Aitkenhead and Chisholm 1982), led to the differentiation on the Derbyshire Carbonate Platform of a flat-topped platform interior region to the west and south and intraplatform basins to the east (Fig. 2a). The

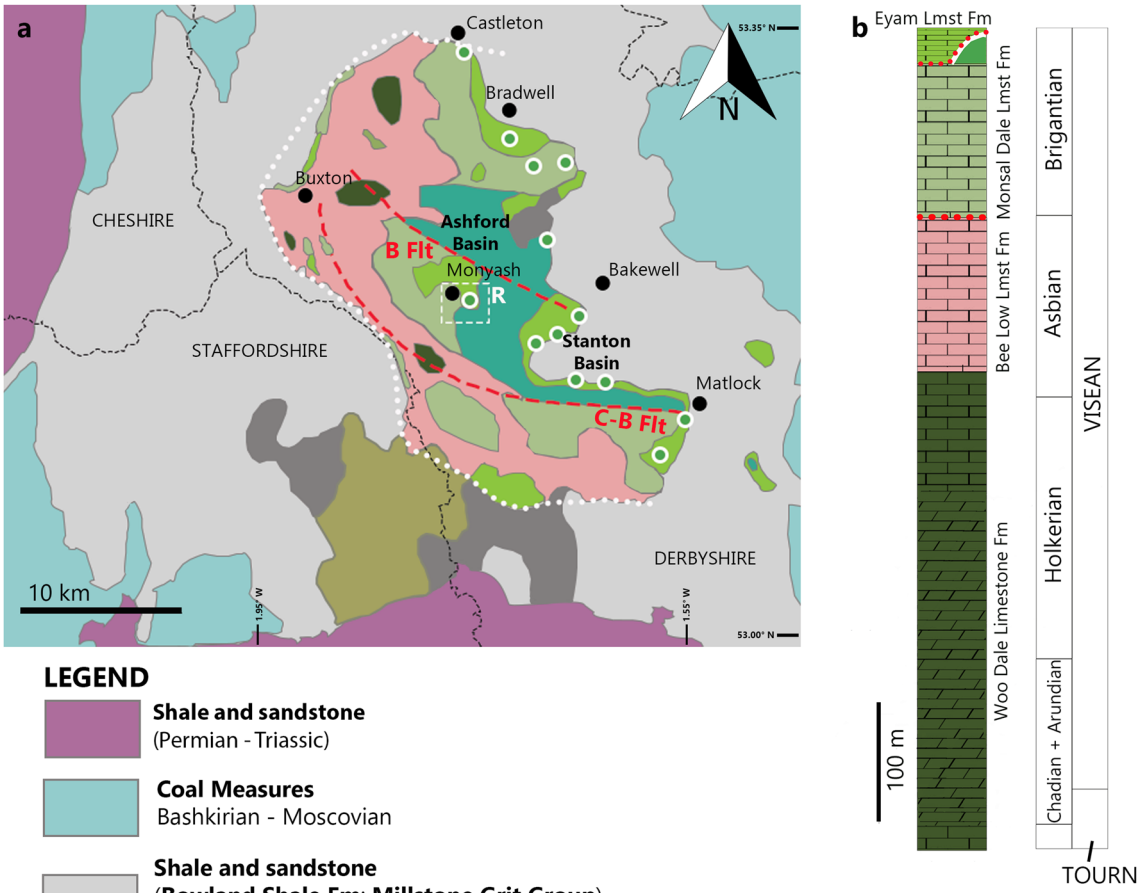

LEGEND

Shale and sandstone
(Permian - Triassic)

Coal Measures
Bashkirian - Moscovian

Shale and sandstone
(**Bowland Shale Fm**; **Millstone Grit Group**)
Serpukhovian - Bashkirian (Namurian)

Widmerpool Formation
upper Visean (Brigantian)

DERBYSHIRE CARBONATE PLATFORM

Eyam Limestone Formation
upper Visean (uppermost Brigantian)

Monsal Dale Limestone Formation
upper Visean (Brigantian)
1. Platform interior; 2. ramp/basin;
3 mud mound.

Bee Low Limestone Formation
upper Visean (middle - upper Asbian)

Woo Dale Limestone Formation
Visean (upper Courceyan - lower Asbian)

Basinal limestones
(**Milldale Lmst, Ecton Lmst, Hopedale Lmst**)
Tournaisian - Visean

1. Limestone; 2. Dolostone

Derbyshire Carbonate Ptl margin
(Asbian, upper Visean)

Fault

Regional subaerial exposure surface

County boundary

Fig. 2 Geological setting of the study area. **a** Simplified geological map of the southern Peak District region. The dashed white box indicates the study area of Ricklow Quarry (R). B Flt—Bakewell Fault; C-B Flt—Cronkston–Bonsall Fault. Modified after Aitkenhead and Chisholm (1982), Gutteridge (1987), Aitkenhead et al. (2002). **b** Stratigraphic column of the study area with regional UK chronostratigraphy, based on data provided by Waters et al. (2009, 2011)

flat-topped platform interior was characterised by the deposition of shallowing-upward 0.5–5 m thick cyclothems (Stevenson and Gaunt 1971; Cox et al. 1977; Aitkenhead et al. 1985; Gutteridge 1987). The restricted intraplatform basins in the east were characterised by low-angle ramp margins and the deposition of various units in normal marine, above and below fair-weather wave base, poorly oxygenated environments, to hypersaline and brackish ponds (Butcher and Ford 1973; Gutteridge 1989a). The north-western margin of the platform in the area of Castleton and to the south of Buxton evolved into a bypass slope dominated by storm-influenced skeletal grainstone shoals (Gawthorpe and Gutteridge 1990; Harwood 2005), whereas the southern margin was a low-angle distally steepened ramp with tidal bars (Gutteridge 2003; Harwood 2005). Sponge-microbial reefs growth halted on the break-in-slope while mud mounds developed on the outer platform (Harwood 2005). Basaltic lava, hyaloclastite, and tuff occur intercalated in the Monsal Dale Limestone Fm (Aitkenhead and Chisholm 1982).

Near the top of the Monsal Dale Limestone Fm, immediately beneath the regional subaerial exposure surface marking the boundary with the overlying Eyam Limestone Formation (Adams 1980; Aitkenhead and Chisholm 1982; Gutteridge 1991) mud mounds ("knoll-reefs" or "reef-knolls" in the older literature; e.g. Smith et al. 1967; Stevenson and Gaunt 1971; Aitkenhead et al. 1985), referable to Bridges et al. (1995) Type 3 buildups developed in the platform interior, margins, and intraplatform ramps (Fig. 2a; Biggins 1969; Orme 1971; Timms 1978; Gutteridge 1995). Mud mounds frequently accreted to form mud mound complexes whose depositional style was affected by the availability of accommodation (Gutteridge 1995): laterally accreted mud mound complexes developed above fair-weather wave base and are hundreds of metres wide, up to 20 m thick; vertically accreted mud mound complexes resulted from the vertical growth of one or a few lens-shaped mud mounds, attaining a thickness up to 50 m (Gutteridge 1995). The mud mound complex at Ricklow Quarry, the focus of this study, is within the laterally accreted group and was interpreted as developed in an intraplatform inner-ramp setting according to Gutteridge (1995), but a middle-ramp setting below fair-weather wave base was proposed by Nolan et al. (2017). Few mud mounds also occur in intraplatform inner-ramp units of the Eyam Limestone Fm (Gutteridge 1995).

Platform growth was terminated by southerly progradation of fluvio-deltaic systems in the early Serpukhovian (Aitkenhead et al. 1985; Guion and Fielding 1988).

The Monsal Dale and Eyam Limestone formations have been traditionally attributed to the Brigantian substage (Ramsbottom in Smith et al. 1967; Mitchell in Stevenson and Gaunt 1971; Fig. 2b). Several studies suggest a correlation of the middle-upper Brigantian of England with the Serpukhovian of the Moscow Basin, mainly based on foraminiferal biozonations (e.g. Sevastopulo and Barham 2014; Vachard et al. 2016; Cózar and Somerville 2014, 2021; Cózar et al. 2019a). However, this study follows Waters et al. (2009, 2011), Aretz et al. (2020), and Lucas et al. (2022) that proposed correlating the upper boundary of the Brigantian with the lower boundary of the Serpukhovian. No biostratigraphic marker of the Serpukhovian occur in the Monsal Dale Limestone Fm of Derbyshire (Nolan et al. 2017; Smith et al. 2017; Carniti et al. 2022).

Materials and methods

The studied mud mound complex crops out to the west of Ricklow Quarry (53° 11′ 30'' N, 01° 45′ 17'' W), near the village of Monyash, Derbyshire, UK (Figs. 2a, 3a). The outcrop is crossed by the Ricklow Dale to the north and Lathkill Dale to the south, resulting in natural sections of its succession and surrounding units (Fig. 3b).

Outcrop investigation, measurement of stratigraphic logs, and petrographic analysis of 57 thin sections with transmitted polarised-light microscope led to the recognition of fifteen lithofacies types. The lithofacies were grouped in lithofacies associations based on depositional texture (cf. Dunham 1962; Embry and Klovan 1971), origin of the carbonate mud (e.g. detrital allomicrite vs. in situ precipitated automicrite), composition of skeletal and non-skeletal grains, bedding character, sedimentary structures, and stratigraphic position. The semi-quantitative proportion of grains in thin sections was determined based on visual estimates and comparison charts for limestone by Baccelle and Bosellini (1965). Spatial distribution of the distinguished lithofacies was determined through lateral tracing between measured stratigraphic logs and outcrops and was reported on a geodatabase built with ArcGIS (Esri®) software based on 1:1,250 topographic maps by Ordnance Survey, containing data about outcrop position, lithofacies classification, strike and dip of beds, major structural features and sample location. The geodatabase was used to extract a lithofacies map of Ricklow Quarry (Fig. 3b). Fossil brachiopod assemblages were collected from the mud mound complex lithofacies. Details about palaeontological sampling and the taxonomy are provided in Carniti et al. (2022). The articulation ratio was calculated based on data from Carniti et al. (2022) as the percentage ratio of articulated specimens to the total number of specimens in each lithofacies association. Bias due to possible uneven distribution of articulated specimens was lowered by considering all

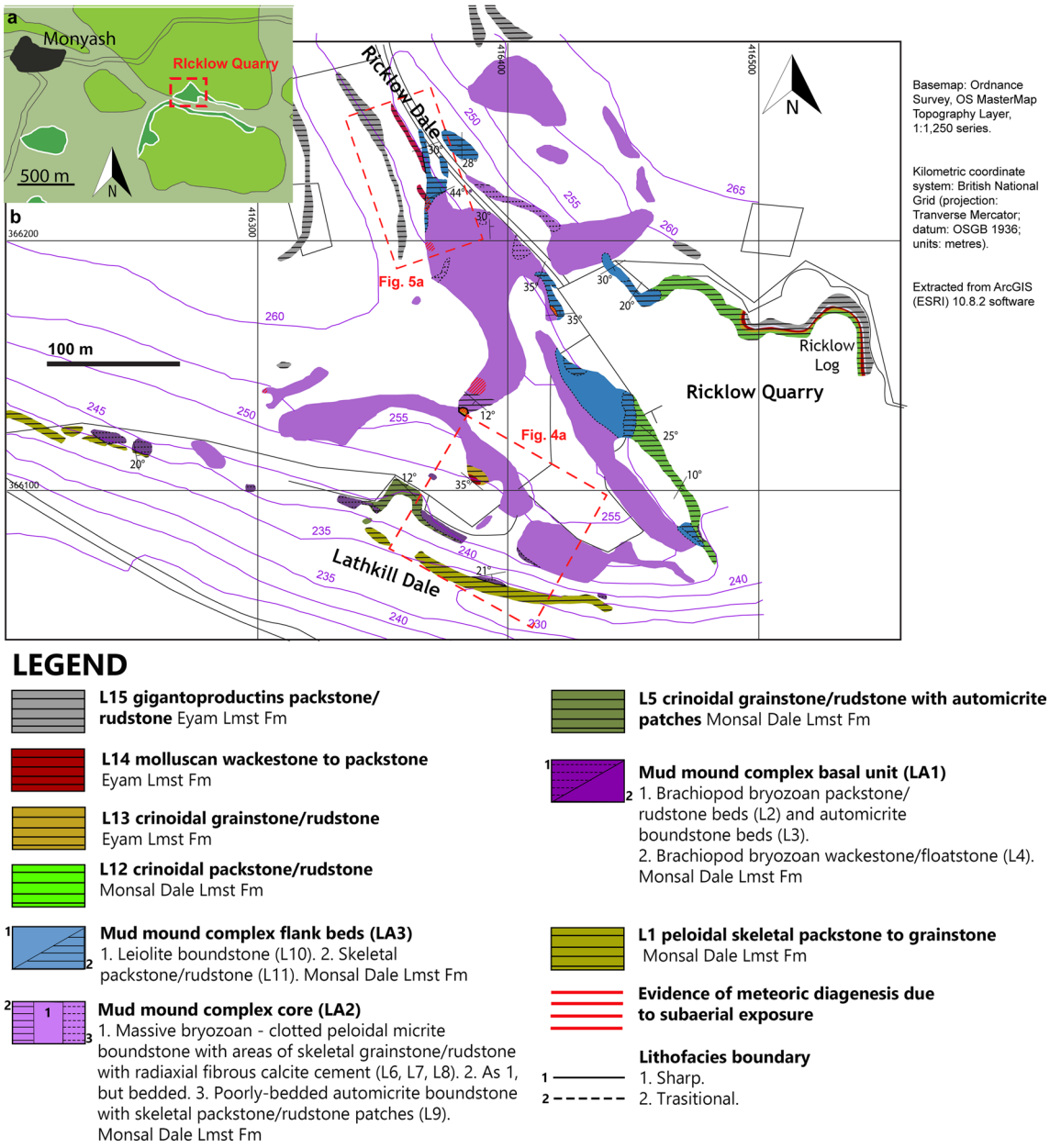

Fig. 3 **a** Geological map of the area around Ricklow Quarry near Monyash, Derbyshire (UK). Modified after British Geological Survey (1978). For legend refer to Fig. 2. **b** Lithofacies map (outcrops only) of the area of the mud mound complex outcrops to the west of Ricklow Quarry, result of this study. The location of the Ricklow Log studied by Nolan et al. (2017) is reported. *L* Lithofacies, *LA* Lithofacies Association

brachiopods from different assemblages collected in the same lithofacies association. Cathodoluminescence analysis was performed on thin sections with a luminoscope CITL Cambridge Image Technology Limited, Cambridge, UK (model MK 5–2 operating system at 10–14 kV with a beam current between 200 and 600 µA, and vacuum gauge 50–70 mTorr) at the University of Milan.

Results

Lithofacies character and architecture

The sedimentary succession investigated at Ricklow Quarry (Figs. 3, 4, 5) consists of a massive convex-upward lens-shaped unit (about 10 m thick) extending laterally for nearly 250 m in an E–W cross section and adjacent to decimetre-thick inclined beds (dips up to 44° with respect

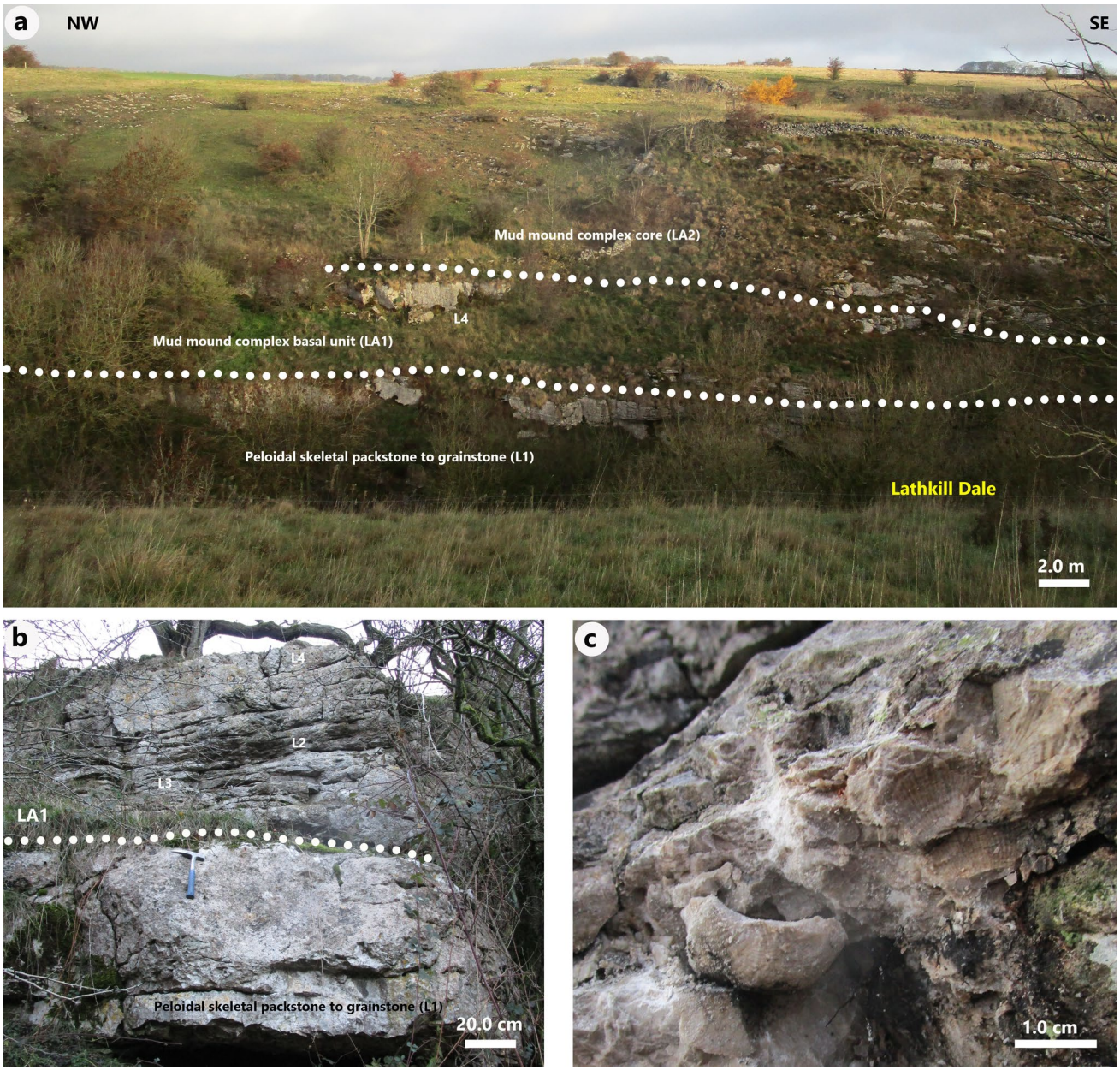

Fig. 4 Field photographs of outcrops in the area of Ricklow Quarry, Monyash, Derbyshire (UK; Fig. 3b). **a** Panoramic view of the north-eastern side of Lathkill Dale showing spatial relationships of the units forming the mud mound complex of Ricklow Quarry. **b** Detail of succession at the base of the mud mound complex of Ricklow Quarry. **c** Detail of a productide specimen (*Antiquatonia hindi* Muir-Wood, 1928) in life position into brachiopod-bryozoan packstone/rudstone beds (L2). L1—peloidal-skeletal packstone to grainstone (pre-mound); L2—brachiopod bryozoan packstone/rudstone beds (LA1); L3—automicrite boundstone beds (LA1); L4—brachiopod bryozoan wackestone/floatstone lens (LA1); LA1—Lithofacies Association 1 (basal unit of the mud mound complex); LA2—Lithofacies Association 2 (mud mound complex core)

to present-day-horizontal), transitional into a horizontally bedded succession (Figs. 4, 5). The massive unit represents the mud mound complex core adjacent to its flank beds. Fifteen lithofacies, L1–L15, described in detail in Table 1, were distinguished as pre-mud mound complex (L1), basal unit of the mud mound complex (L2–L4), mud mound complex core (L6–L9), inclined flank beds (L10, L11), lateral to off-mud mound complex strata (L5, L12), and strata overlying the mud mound complex (L13–L15). The lithofacies association (LA1–LA3) characteristics are summarised in Table 2.

Lithofacies L1: peloidal–skeletal packstone to grainstone forms 50–100 cm thick horizontal planar beds (Fig. 4a, b)

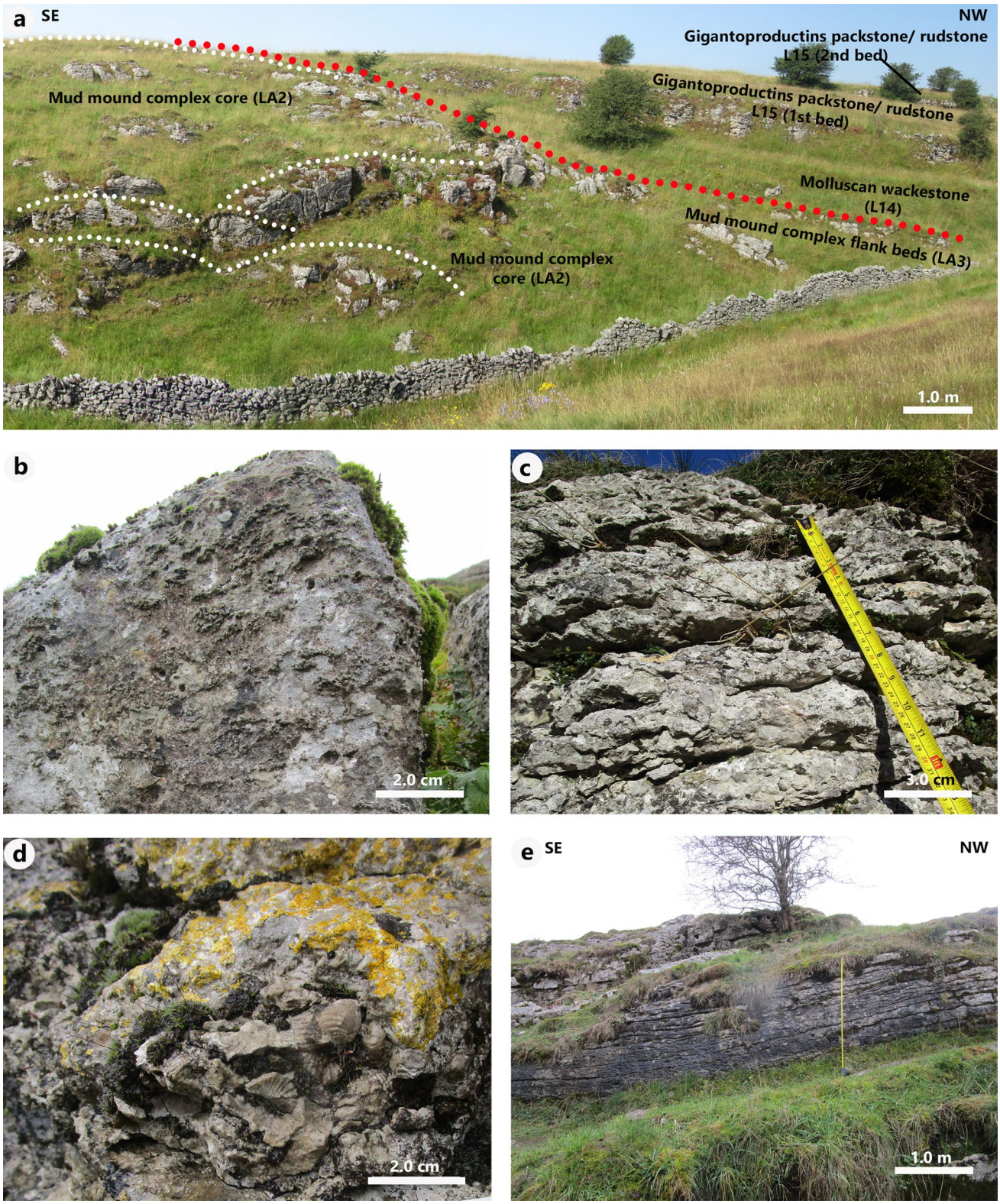

and represents the lowest stratigraphic unit cropping out in the southern portion of the study area, in Lathkill Dale (Fig. 3b). L1 includes sparse, fragmented, and micritised crinoid ossicles, benthic foraminifers, and rare "black pebbles" (cf. Flügel 2004; Fig. 6a, b).

L1 beds are overlain by a 10 m thick succession of 3–5 cm thick nodular, sub-horizontal beds of brachiopod

◂**Fig. 5** Field photographs of outcrops in the area of Ricklow Quarry, Monyash, Derbyshire (UK; Fig. 3b). **a** Panoramic view of mud mound complex core (Lithofacies Association 2—LA2) with inclined flank beds (Lithofacies Association 3—LA3), capped by subaerial exposure surface (red dashed line). The mud mound complex is onlapped by molluscan wackestone to packstone (L14) and gigantoproductins packstone/rudstone beds (L15). The mud mound complex core consists of numerous metre-scale lens-shaped massive convex-upward units (white dashed lines). **b** Detail of massive mud mound complex core outcrop (LA2) showing numerous silicified brachiopods and micrite patches protruding from the weathered outcrop surface. **c** Detail of irregular sub-horizontal beds of automicrite boundstone with skeletal packstone/rudstone patches into the mud mound complex core (L9, LA2). **d** Detail of rhynchonellide articulated brachiopods (*Pleuropugnoides pleurodon* Phillips, 1836) in the irregular beds of automicrite boundstone of L9 (LA2). **e** Inclined flank beds (30° inclination with respect to present-day-horizontal; LA3)

bryozoan packstone/rudstone (L2), irregularly interbedded and laterally transitional within a few decimetres to L3 sparsely fossiliferous automicrite boundstone. Lithofacies L3 forms 5–8 cm thick tabular beds or lenses with a diameter and thickness of 10 cm (Fig. 4b). Both L2 and L3 contain common brachiopods, sparse bryozoans, bivalves, crinoids, calcite-replaced originally siliceous sponge spicules, clotted peloidal micrite intraclasts (Fig. 6c), and millimetre-size equidimensional to elongated nodules of clotted peloidal micrite to leiolite with isoriented sponge spicules (Fig. 6d). L2 contains millimetre-size patches of clotted peloidal micrite to leiolite forming 10% of the rock volume, while in L3 automicrite dominates the rock volume (Fig. 6e, f): clotted peloidal micrite (peloids 0.05–0.1 mm in diameter) passes within few millimetres into leiolite (Fig. 7a), locally forming a regular alternation of millimetre-size levels of leiolite and clotted peloidal micrite (Fig. 7b). Millimetre- to centimetre-size, automicrite supported primary voids are filled by blocky calcite cement and addressed as stromatactis-like cavities because of their shape resemblance with stromatactis cavities (Dupont 1881; Bourque and Boulvain 1993; Tsien 1985).

Thick, poorly bedded to massive lenses (up to 1 m thick, 5–6 m wide) of brachiopod–bryozoan wackestone/floatstone (L4) occur interbedded in the succession formed by L2 and L3 (Fig. 4b). L4 also contains sparse crinoids, ostracods, and sponge spicules (Fig. 7c, d), and it is associated with millimetre-size patches of automicrite boundstone similar to L3 (30% of rock volume; Fig. 7e, f).

The association of L2 and L3 beds with L4 lenses builds the basal tabular unit of the mud mound complex, which is considered as Lithofacies Association 1 (LA1; Fig. 3b; Table 2). Brachiopods are the dominant macrofossils in LA1: specimens are both articulated and not articulated (articulation ratio 37.8%), commonly not in life position. Some productides occur in life position, with articulated spines, at the base of beds (Fig. 4c). A brachiopod faunal list for unit LA1 is given in Table 3. LA1 unit is adjacent to 8–40 cm thick horizontal massive beds of crinoidal grainstone/rudstone with automicrite patches (L5), with sparse bryozoans, brachiopods, and automicrite intraclasts (Figs. 3b, 8a–b).

The LA1 passes upwards to a 10 m thick association of massive lens-shaped units with a thickness of 1–2 m and a diameter of 4–5 m; the units laterally and vertically accrete to form decametre-scale lens-shaped convex-up mud mounds (Figs. 3b, 5a, b). Individual mud mounds coalesced to form the mud mound complex; however, in some areas, the buildup appears as an undifferentiated massive object and the composite nature is not recognisable. The lens-shaped units consist mainly of millimetre- to decimetre-size patches of clotted peloidal micrite boundstone (L7; 60% rock volume), chaotically mixed with minor fenestellid bryozoan boundstone/cementstone (L6; 10% rock volume), with skeletal grainstone/rudstone filling the primary voids in-between the patches (L8; 30% rock volume).

L6 is dominated by non-luminescent, isopachous radiaxial fibrous calcite cement filling the voids among the upright growth of fenestellid fronds and forming 40–50% of rock volume (Fig. 9a–c). L7 consists of millimetre- to decimetre-size patches of clotted peloidal micrite with < 0.5 mm peloids into a mosaic of microsparite, with sparse brachiopods and sponge spicules (Fig. 9d, e). Primary cavities in the clotted peloidal micrite patches are few and small (0.5–2 mm; Fig. 9f). L7 patches alternate with minor irregular millimetre- to decimetre-size volumes filled by L8 skeletal grainstone/rudstone (Fig. 10a), where common bryozoan fragments, brachiopods, and sparse automicrite intraclasts occur within microsparite with sparse sub-millimetric peloids, and radiaxial fibrous calcite cement (forming 30% rock volume; Fig. 10b, c). L7 passes to L8 with an irregular boundary, both sharp, lined by fibrous calcite cement, or transitional (Fig. 10d).

Also, in the mud mound complex core there are decimetre- to metre-size volumes of poorly defined, laterally discontinuous, 5–15 cm thick sub-horizontal beds (Fig. 5c, d) formed by automicrite boundstone with patches of packstone/rudstone forming up to 30–40% rock volume (L9). Skeletal content is higher than in L7 (Fig. 10e, f). Irregular volumes filled by a bryozoan fragment grainstone similar to L8 are more abundant then in L7 (20% rock volume).

The association of L6, L7, L8 massive lens-shaped units and L9 irregularly bedded areas building the mud mound complex core is considered as Lithofacies Association 2 (LA2; Fig. 3b). Brachiopods are the dominant macrofossils and are widespread in mud mound complex core. They are commonly articulated (articulation ratio 56.8%). Locally, silicified brachiopod shells and millimetre- to centimetre-size microquartz patches protrude from the weathered outcrop surface (Fig. 5b). A high density of specimens occurs in decimetre-size lenses dominated by L8 (more than twenty in a volume of 0.5 dm^3), passing gradually to more sparsely

Table 1 Description of the lithofacies of the study area of Ricklow Quarry

Lithofacies type	Texture	Skeletal grains	Non-skeletal grains	Bedding and sedimentary structures	Diagenetic features	Depositional environment	Lithofacies association (LA)
L1—peloidal-skeletal packstone to grainstone	Packstone to grainstone. Fine–medium sand-grained (0.05–1.0 mm); well-sorted. Very rare Rhynchonellata shells up to 15 mm in diameter	Fragmented and abraded skeletal grains. Crinoid ossicles (S); benthic foraminifers: endothyrids (*Endothyra*, *Endothyranella*) (S), cf. *Spireitlina* (R), globivalvulinids (*Biseriella*) (VR), earlandiids (*Paratikhinella tenuis* Conil, 1980) (VR), archeodiscides (VR), textulariids (VR); brachiopods: Rhynchonellata fibrous and minor Strophomenata laminar shell fragments (R); calcispheres (R); bivalve shells (VR); echinoid spines (VR); monoaxone calcified siliceous sponge spicules (VR); putative algal fragments (VR)	Peloids (C); dark red or black lithoclasts ("black pebbles") (R); chalcedony extraclasts (VR); micrite intraclasts (0.05–0.1 mm in diameter) (R)	50–100 cm thick massive horizontal planar beds	Skeletal grains are heavily micritised (particularly crinoids and foraminifers). Compaction: point to long grain contacts. Intra- and intergranular porosity filled by luminescent recrystallized allomicrite, dull-luminescent burial blocky and syntaxial calcite cements. The entire texture was recrystallized as shown by widespread dull luminescence, unless for some non-luminescent crinoid ossicles. Fissures and dissolution vugs are few and filled by bright-luminescent late-burial blocky calcite cement	Open-marine subtidal inner-ramp environment	Lithofacies underlying the mud mound complex (pre-mud mound)
L2—brachiopod bryozoan packstone/rudstone	Packstone with mm-size patches of clotted peloidal micrite (densely packed peloids, 0.05–0.1 mm in diameter) to leiolite (10% rock volume). Medium sand–cobble-grained (0.2–80 mm); unsorted	Brachiopods: shells of productides and spiriferides, minor terebratulides, rhynchonellides, orthides (C), productide spines (R); bryozoans: fenestellid (S), fistuliporid (R), ramose (VR); crinoid ossicles (S); bivalve shells (R); monoaxone calcified siliceous sponge spicules (R); benthic foraminifers: endothyrids (*Mikhailovella*), tetrataxids (*Tetrataxis*), earlandiids (*Earlandia tenuis*), archeodiscides (VR); calcispheres (VR); echinoid plates (VR); ostracods (VR); trilobites (VR)	Nodules of clotted peloidal micrite (mm-size; with isoriented monoaxone calcified siliceous sponge spicules) (S); intraclasts of clotted peloidal micrite (S)	3–5 cm thick nodular, irregular, sub-horizontal beds. Slight skeletal grain isorientation in the packstone	Productide spines show microborings, some crinoid ossicles are micritised. Compaction: point contacts. Intergranular and intragranular porosity filled by luminescent re-crystallised allomicrite and luminescent burial blocky calcite cement. Stromatactis-like primary cavities (1–1.5 mm) in the automicrite filled by burial calcite cement. Intragranular porosity filled by meteoric phreatic non-luminescent blocky calcite cement. Few dissolution vugs and fissures, filled by luminescent burial blocky calcite cement. All the texture was recrystallized as shown by widespread luminescence of all grains, except for spiriferide brachiopod shells and blocky calcite cement in intragranular pores. Clotted peloidal micrite intraclasts show a dull luminescence unless for calcitized spicules, which are bright	Low- to moderate-energy, middle-ramp environment	LA1—mud mound complex basal unit

Table 1 (continued)

Lithofacies type	Texture	Skeletal grains	Non-skeletal grains	Bedding and sedimentary structures	Diagenetic features	Depositional environment	Lithofacies association (LA)
L3—automicrite boundstone	Clotted peloidal micrite (densely to loosely packed peloids, 0.05–0.1 mm in diameter with microsparite) to leiolite boundstone with mm-size patches of skeletal packstone (10% rock volume). Leiolite passes to clotted peloidal micrite in some mm showing in some cases cyclic alternations of 3.0–5.0 mm thick leiolite levels and densely to loosely packed peloidal micrite levels. Medium sand–gravel-grained (0.2–60 mm); unsorted	Articulated brachiopods: mainly productide and spiriferide, minor terebratulide, rhynchonellide, orthide shells (S–C), productide spines (R–S); bryozoans: fenestellid (S), ramose (S), fistuliporid (R); disarticulated bivalve shells (S), bivalve moulds (VR); crinoid ossicles (S); monoaxone calcified siliceous sponge spicules (S); ostracods (R); benthic foraminifers: endothyrids, palaeotextulariids, tuberitinids (*Tuberitina*) (VR); calcispheres (VR); gastropods (VR)	Nodules of clotted peloidal micrite (mm-size; with isoriented monoaxone calcified siliceous sponge spicules) (S); intraclasts of clotted peloidal micrite (R); phosphate grains (VR)	5–8 cm thick tabular beds and lens-shaped, convex-up units, 10 cm in diameter. Packstone patches show slight skeletal grain isorientation	Some brachiopod shells are micritised and show microborings. Compaction: point contacts. Few, short (1.0–2.0 mm) stylolites filled by reddish bitumen. Intergranular and intragranular porosities filled by luminescent recrystallized automicrite, allomicrite, non-luminescent meteoric or marine syntaxial calcite and luminescent burial blocky calcite cement. Few stromatactis-like primary cavities (1.0–3.0 mm) filled by burial blocky calcite cement. Irregular dissolution vugs enlarging primary cavities (3.0–5.0 mm) filled by luminescent late-burial blocky calcite cement. All the rock was recrystallized as shown by luminescence of grains unless for spiriferide brachiopod shells	Low- to moderate-energy, middle-ramp environment	LA1—mud mound complex basal unit
L4—brachiopod bryozoan wackestone/floatstone	Wackestone to packstone, chaotically mixed, with mm-size automicrite boundstone (mainly leiolite) similar to L3. Automicrite boundstone is 30% of rock volume. Medium sand–gravel-grained (0.2–60 mm); unsorted	Skeletal grains are fragmented and disarticulated. Brachiopods: mainly productide, minor spiriferide and terebratulide shells (C), productide spines (S); bivalve shells (S); bryozoans: fenestellid (S), fistuliporid (R), ramose (R); crinoid ossicles (S); ostracods (S); monoaxone calcified siliceous sponge spicules (S); calcispheres (R); benthic foraminifers: endothyrids (small cf. *Endothyranopsis*; *Omphalotis*), textulariids, archeodiscides (*Archeodiscus, Pararcheodiscus, Tubispirodiscus*), tuberitinids (*Tuberitina*) (VR); echinoid plates (VR); bivalve moulds (VR); possible crustacean fragments (VR); trilobites (VR)	Clotted peloidal micrite intraclasts (mm-size; peloids 0.05–0.1 mm in diameter) (S); phosphate grains (VR)	Poorly bedded lenses, 100 cm thick and 500–600 cm wide. Isoriented skeletal grains in the wackestone–packstone	Some skeletal grains show microborings and micritisation. Compaction: long and sutured grain contacts; few, short (1.0–2.0 mm) stylolites with bitumen. Intergranular and intragranular porosities filled by bright-luminescent recrystallized allomicite and dull-luminescent recrystallized automicrite, non-luminescent meteoric phreatic isopachous dogtooth calcite and luminescent burial blocky calcite cements. Few stromatactis-like to irregular primary cavities (3.0–5.0 mm) filled by burial blocky calcite cement. Irregular dissolution vugs and fissures enlarging primary cavities (5.0–10.0 mm), filled by silt-size vadose pedogenised material and luminescent late blocky calcite cement. Silicification incipit in some brachiopod shells. All the texture was recrystallized as shown by widespread luminescence of grains, except for some brachiopod shells	Low- to moderate-energy, middle-ramp environment	LA1—mud mound complex basal unit

Table 1 (continued)

Lithofacies type	Texture	Skeletal grains	Non-skeletal grains	Bedding and sedimentary structures	Diagenetic features	Depositional environment	Lithofacies association (LA)
L5—crinoidal grainstone/rudstone with automicrite patches	Grainstone to packstone with mm-size patches of leiolite to clotted peloidal micrite (10% rock volume). Coarse sand–cobble-grained (1.0–100.0 mm); moderately sorted	Crinoid ossicles, stems and fragments (VC); bryozoans: ramose (S), fenestellid (R), fistuliporid (R); brachiopods: Strophomenata laminar and Rhynchonellata fibrous shell fragments (S), productide spines (R); monoaxone calcified siliceous sponge spicules (in automicrite patches) (S); benthic foraminifers: archeodiscides (cf. *Pseudoammodiscus;* cf. *Asteroarcheodiscus*; *Planoarcheodiscus*), endothyrids (small cf. *Endothyranopsis*; *Omphalotys*) (VR), tetrataxids (*Tetrataxis*), palaeotextulariids, tuberitinids (*Tuberitina*) (VR); bivalve shells (VR); calcispheres (VR); gastropods (VR); ostracods (VR)	Nodules of clotted peloidal micrite (peloids 0.05–0.1 mm in diameter with microsparite) to leiolite (mm-size; with isoriented monoaxone calcified siliceous sponge spicules) (S)	8–40 cm thick horizontal beds with isoriented grains	Skeletal grains are frequently micritised. Compaction: long and concavo-convex contacts. Few stylolites are present and filled by bitumen. Intergranular porosity filled by luminescent re-crystallised allo- and automicrite, non-luminescent meteoric or marine syntaxial cement with luminescent burial overgrowths, and luminescent zoned burial blocky calcite cement. Intragranular porosity with geopetal fillings and luminescent burial blocky calcite cement. Dissolution vugs and fissures filled by bright-luminescent late-burial blocky calcite cement. All the texture was recrystallized as shown by widespread luminescence of skeletal grains, except for some crinoid ossicles, brachiopod shells, and automicrite intraclasts	Low- to moderate-energy, middle-ramp environment. Representing off-mud mound complex deposition during the initial stages of mud mound complex growth	Off-mud mound complex lithofacies
L6—fenestellid bryozoan boundstone/cementstone	Bryozoan boundstone/cementstone. Radiaxial fibrous calcite cement 40–50% of rock volume. Medium sand–gravel-grained (0.2–60 mm); unsorted	Bryozoans: entire fenestellid fronds (VC), fistuliporid (R); brachiopods: mm-size spiriferide and terebratulide shells (R), productide spines (VR–S); benthic foraminifers: tuberitinids (*Tuberitina*) (VR); bivalve shells (VR); crinoid ossicles (VR); gastropods (VR); monoaxone/triaxone calcified siliceous sponge spicules (in automicrite patches) (VR); ostracods (VR)	Clotted peloidal micrite intraclasts (peloids < 0.05 mm in diameter) (R)	Massive, lens-shaped, convex-up units, 1–2 m thick, 4–5 m in diameter	Compaction: sutured contacts, stylolites (with bitumen). Intergranular and intragranular porosities filled by luminescent recrystallised clotted peloidal micrite, luminescent recrystallized isopachous radiaxial fibrous marine calcite cement, non-luminescent meteoric phreatic dog-tooth calcite cement, luminescent blocky calcite cement. Some megaquartz and chalcedony present due to silicification. Fissures are filled by luminescent late-burial blocky calcite cement or bitumen. All texture is recrystallized as shown by luminescence of grains	Low- to moderate-energy, middle-ramp environment. Areas of the mud mound complex core dominated by fenestellid bryozoans	LA2—mud mound complex core

Table 1 (continued)

Lithofacies type	Texture	Skeletal grains	Non-skeletal grains	Bedding and sedimentary structures	Diagenetic features	Depositional environment	Lithofacies association (LA)
L7—clotted peloidal micrite boundstone	Boundstone dominated by mm- to dm-size patches of clotted peloidal micrite (densely to loosely packed peloids, < 0.05 mm in diameter, with microsparite; minor volumes dominated by microsparite) surrounded by isopachous radiaxial fibrous calcite cement. Irregular volumes (mm-size) with fenestellid bryozoan fronds and brachiopod spines with radiaxial fibrous calcite in-between (20% rock volume). Minor leiolite mm-size patches (5% rock volume). Medium sand–gravel-grained (0.2–60 mm); unsorted	Brachiopods: productide and minor spiriferide, terebratulide, rhynchonellide shells (S), productide spines (S); monoaxone calcified siliceous sponge spicules (R–S); bryozoans: fenestellid (R), fistuliporid (VR), ramose (VR); bivalve shells (R); calcispheres (R); crinoid ossicles (R); ostracods (R); benthic foraminifers: endothyrids (small cf. *Endothyranopsis*, *Endothyranopsis*), palaeotextulariids, tetrataxids (*Tetrataxis*), archeodiscides (*Pseudoammodiscus*), tuberitinids (*Tuberitina*) (VR); gastropods (VR); goniatites (VR)	Leiolite intraclasts (R); phosphate grains (VR)	Massive, lens-shaped, convex-up units, 1–2 m thick, 4–5 m in diameter	Some skeletal grains with microborings. Compaction: linear to sutured contacts. Intergranular and intragranular porosities filled by non-luminescent marine isopachous radiaxial fibrous calcite cement, non-luminescent marine or meteoric syntaxial calcite cement, brownish non-luminescent meteoric vadose pendant calcite cement, non-luminescent meteoric dogtooth prismatic calcite cement, luminescent burial blocky calcite cement, minor megaquartz cement. Very few irregular primary cavities (0.5–2.0 mm) filled by burial blocky calcite cement. Microquartz in some portions of the matrix and brachiopod valves as the result of silicification. Dissolution of matrix and grains is widespread: vugs and fissures are filled by luminescent late-burial blocky calcite cement. All the texture was recrystallized as revealed by widespread luminescence of grains, unless for some clotted peloidal micrite patches and brachiopod shells	Low- to moderate- energy, middle-ramp environment. Areas of the mud mound complex core with siliceous sponges, fenestellid bryozoans, and brachiopods	LA2—mud mound complex core
L8—skeletal grainstone/rudstone	Grainstone with abundant radiaxial fibrous calcite cement (20–30% in volume) and microsparite with sparse peloids (0.1 mm in diameter). Medium sand–gravel-grained (0.2–60 mm); unsorted	Brachiopods: mainly productide and spiriferide shells (C), productide spines (S); bryozoans: fenestellid frond fragments (C); crinoid ossicles (R); monoaxone calcified siliceous sponge spicules (in leiolite patches) (R); ostracods (R); benthic foraminifers: endothyrids, tuberitinids (*Tuberitina*) (VR)	Clotted peloidal micrite (mm-size; peloids < 0.05 mm in diameter) to leiolite intraclasts (S); phosphate grains (VR)	Massive, lens-shaped, convex-up units, 1–2 m thick, 4–5 m in diameter	Some skeletal grains show microborings. Compaction: point and linear contacts. Intergranular and intragranular porosities filled by clotted peloidal micrite mixed with microsparite, luminescent re-crystallised marine isopachous radiaxial fibrous calcite, non-luminescent meteoric phreatic dogtooth and equant calcite cements, luminescent burial blocky calcite cement. Microquartz due to silicification of the matrix and some crinoid ossicles. Dissolution vugs filled by luminescent late-burial blocky calcite cement	Low- to moderate- energy, middle-ramp environment. L8 represents the filling in-between L7 and L9 boundstone mm- to dm-size patches	LA2—mud mound complex core

Table 1 (continued)

Lithofacies type	Texture	Skeletal grains	Non-skeletal grains	Bedding and sedimentary structures	Diagenetic features	Depositional environment	Lithofacies association (LA)
L9—automicrite boundstone with skeletal packstone/rudstone patches	Leiolite to clotted peloidal micrite (densely to loosely packed peloids, < 0.05 mm in diameter, with microsparite) boundstone with mm- to cm-size patches of packstone (30–40% rock volume). Automicrite in mm-size patches is surrounded by isopachous radiaxial fibrous calcite cement, adjacent to volumes dominated by microsparite with peloids and radiaxial fibrous calcite with bryozoan debris (20% rock volume), and patches of skeletal packstone. Medium sand–gravel-grained (0.2–60 mm); unsorted	Fragmented skeletal grains. Brachiopods: mainly productide, minor rhynchonellide, terebratulide, spiriferide shells (S–C), productide spines (R); monoaxone calcified siliceous sponge spicules (dominant in leiolite and wackestone) (S–C); bryozoans: fenestellid fragments (S), fistuliporid (R); crinoid ossicles (S); ostracods (S); benthic foraminifers: endothyrids, archeodiscides, tuberitinids (*Tuberitina*) (VR); crustacean fragments (VR)	Clotted peloidal micrite intraclasts (mm-size; peloids < 0.05 mm in diameter) (S)	Massive to poorly bedded: 5–15 cm thick irregular subhorizontal beds. Skeletal grains slightly isoriented, in particular in packstone patches	Some skeletal grains show microborings. Compaction: point and linear contacts; stylolites are common, intersecting at least two families of fissures; they are filled by bitumen. Intergranular and intragranular porosities and irregular primary cavities (mm-size) filled by luminescent recrystallized allomicrite and automicrite, non-luminescent marine isopachous radiaxial fibrous calcite cement and luminescent burial blocky calcite cement. Secondary dissolution vugs filled by blocky calcite cement and bitumen. All the rock was recrystallized as revealed by widespread luminescence (except for some brachiopod shells)	Low- to moderate-energy, middle-ramp environment. L9 represents areas dominated by bryozoans and brachiopods in the mud mound complex core	LA2—mud mound complex core
L10—leiolite boundstone	Leiolite, minor clotted peloidal micrite (densely to loosely packed peloids, < 0.05 mm in diameter, with microsparite) boundstone with mm- to cm-size patches of burrowed wackestone (30–40% rock volume). Medium sand-grained with some gravel-size skeletal grains (0.2–60 mm); poorly sorted	Fragmented skeletal grains. Brachiopods: mainly productide and orthide, minor rhynchonellide, spiriferide and terebratulide shells (S), productide spines (R), reworked shells (VR); monoaxone/tetraxone calcified siliceous sponge spicules (in leiolite boundstone) (S); bryozoans: fenestellid fragments (S), ramose (R); bivalve moulds (R); crinoid ossicles (R–S); crustacean fragments (R); goniatites (R); ostracods (R); benthic foraminifers: endothyrids, archeodiscides (?*Pseudoammodiscus*), tuberitinids (*Tuberitina*) (VR)	Clotted peloidal micrite intraclasts (mm-size; peloids < 0.05 mm in diameter) (S)	Massive to poorly bedded: 100 cm thick inclined beds (up to 44°) Isorientation of grains poor to evident in wackestone patches. Bioturbation in allomicrite	Some skeletal grains are micritised. Compaction: point and linear contacts; many irregular stylolites (filled by bitumen). Intergranular and intragranular porosities and very few irregular primary cavities (mm-size) filled by allomicrite, automicrite, and luminescent burial blocky calcite cement. Pervasive dissolution: voids filled by luminescent late-burial blocky calcite cement and bitumen	Low- to moderate-energy, middle-ramp environment, in the transitional zone between the mud mound complex core and the off-mud mound complex areas	LA3—mud mound complex flank beds

Table 1 (continued)

Lithofacies type	Texture	Skeletal grains	Non-skeletal grains	Bedding and sedimentary structures	Diagenetic features	Depositional environment	Lithofacies association (LA)
L11—skeletal packstone/ rudstone	Packstone with patches of clotted peloidal micrite. Medium sand–gravel-grained (0.2–60 mm); unsorted	Fragmented skeletal grains. Brachiopods: productide, terebratulide, spiriferide shells (C), productide spines (S); bryozoans: fenestellid, fistuliporid and ramose, each of which may dominate on others in abundance (C); crinoid ossicles (C); ostracods (C); bivalve shells (S); monoaxone calcified siliceous sponge spicules (in automicrite patches) (S–R); benthic foraminifers: endothyrids (*Omphalotys*), tetrataxids (*Tetrataxis*), archeodiscides, tuberitinids (*Tuberitina*) (VR); echinoid plates (VR); trilobite fragments (VR)	Clotted peloidal micrite to leiolite intraclasts (S)	10–50 cm thick inclined beds (8–35°) with isoriented skeletal grains	Skeletal grains show frequently microborings. Compaction: point and linear contacts; stylolites (filled by bitumen). Intergranular and intragranular porosities filled by allomicrite, few luminescent recrystallized marine radiaxial fibrous calcite cement, luminescent burial syntaxial and blocky calcite cements. Widespread dissolution: voids are filled by luminescent late-burial blocky calcite cement and bitumen	Low- to moderate-energy, middle-ramp environment in the transitional zone between the mud mound complex core and the off-mud mound complex areas	LA3—mud mound complex flank beds
L12—crinoidal packstone/ rudstone	Packstone to grainstone with mm-size patches of wackestone (15% rock volume). Coarse sand-grained with cobble-size crinoid ossicles and stems (1.0–100 mm); moderately sorted	Some skeletal grains fragmented, not abraded. Skeletal debris in wackestone patches. Crinoid ossicles and stems (VC); brachiopods: Rhynchonellata fibrous and Strophomenata laminar shells (C), productide spines (S); ostracods (R); calcispheres (R); bryozoans: fenestellid (C), fistuliporid (R); monoaxone calcified siliceous sponge spicules (mainly in wackestone patches) (R); benthic foraminifers: endothyrids, tetrataxids (*Tetrataxis*), tuberitinids (*Tuberitina*) (VR); echinoid plates and spines (VR); palaeoberesellid algae debris (VR)	Intraclasts (mm-size) of clotted peloidal micrite (peloids < 0.1 mm in diameter with microsparite) to leiolite (with monoaxone calcified siliceous sponge spicules and ostracods) (S); peloids (R); phosphate grains (VR)	20–50 cm inclined (10–25°) beds with poorly isoriented skeletal grains	Productide spines are abundantly microbored. Compaction: sutured contacts and stylolites. Intergranular and intragranular porosities filled by allomicrite, minor clotted peloidal micrite and microsparite, non-luminescent marine or meteoric syntaxial calcite cement with luminescent burial overgrowths, luminescent blocky calcite cement. Silicification: microcrystalline quartz on brachiopod shells. Dissolution vugs and fissures filled by blocky calcite cement. Stylolites and fissures are filled by bitumen	Low- to moderate-energy, middle-ramp environment. Representing off-mud mound complex deposition during the mud mound complex core growth	Off-mud mound complex facies

Table 1 (continued)

Lithofacies type	Texture	Skeletal grains	Non-skeletal grains	Bedding and sedimentary structures	Diagenetic features	Depositional environment	Lithofacies association (LA)
L13—crinoidal grainstone/rudstone	Grainstone. Coarse sand–gravel-grained (1–50 mm), moderately well-sorted	Crinoid ossicles (VC); brachiopods: Strophomenata laminar and impunctate Rhynchonellata fibrous shells (S), productide spines (S); bryozoans: fenestellid (R), ramose (R); calcispheres (R); benthic foraminifers: endothyrids (*Omphalotis)*, palaeotextulariids, tetrataxids (*Tetrataxis*), archeodiscides (*Archeodiscus*) (R)	Peloids (R); angular intraclasts of clotted peloidal micrite (with monoaxone calcified siliceous sponge spicules) (R); phosphate grains (VR)	Horizontal to inclined (up to 35°) beds with a thickness of 5–40 cm	Some skeletal components show endolith perforations. Compaction: linear to concavo-convex contacts. Intergranular and intragranular porosities filled by minor luminescent recrystallized allomicrite, non-luminescent meteoric pendant calcite cement, luminescent burial syntaxial and blocky calcite cement. Fissures filled by bitumen. Micrite is recrystallized as shown by its luminescence	High-energy, inner-ramp environment. Crinoid-rich skeletal grainstone subaqueous dunes onlapping the mud mound complex	Post mud mound complex facies
L14—molluscan wackestone to packstone	Wackestone to packstone. Medium sand–gravel-grained (0.2–50 mm); poorly sorted	Disarticulated and fragmented skeletal grains. Bivalve moulds and shells (C); monoaxone calcified siliceous sponge spicules (S); benthic foraminifers: endothyrids (*Endothyranopsis*), palaeotextulariids, tuberitinids (*Tuberitina*) (R); brachiopods: Rhynchonellata fibrous and Strophomenata laminar shells (S), productide spines (R); fenestellid bryozoans (R); calcispheres (R); palaeoberesellid algae debris (R); ostracods (R)	Peloids (S); phosphate grains (VR)	50 cm thick sub-horizonal to inclined (up to 35°), with isoriented skeletal grains	Some skeletal grains show microborings. Compaction: point to long contacts; stylolites. Intergranular porosity filled by luminescent recrystallized allomicrite and luminescent burial blocky calcite cement. Mouldic and intragranular porosities filled by clotted peloidal micrite, geopetal filling or blocky calcite cement. All the rock was recrystallized as shown by widespread luminescence	Low-energy restricted subtidal lagoonal environment sheltered by mud mound complex vestigial topography	Post mud mound complex facies

Table 1 (continued)

Lithofacies type	Texture	Skeletal grains	Non-skeletal grains	Bedding and sedimentary structures	Diagenetic features	Depositional environment	Lithofacies association (LA)
L15—gigantoproductins packstone/rudstone	Packstone to wackestone. Cobble-grained (1–120 mm); moderately well-sorted	Brachiopods: mainly *Gigantoproductus* shells (VC); crinoid ossicles (S); benthic foraminifers: endothyrids (small cf. *Endothyranopsis*, *Omphalotys*), bradyinids, earlandiids (*Earlandia vulgaris* Rauzer-Chernousova and Fursenko, 1937), eostaffellids (*Eostaffella*), palaeotextulariids, tetrataxids (*Tetrataxis*), tuberitinids (*Tuberitina*) (R); ostracods (R); echinoid plates and spines (VR); bivalve shells (VR); bryozoans: fenestellid (VR); calcispheres (VR); gastropods (VR); palaeoberesellid algae debris (VR); red algae (?*Ungdarella*, ?*Fasciella*) (VR); rugose corals (VR); trilobites (VR)	Peloids (S); phosphate grains (R)	100–200 cm thick subhorizontal nodular beds	Some skeletal grains are fragmented by mechanical compaction. Compaction: sutured contacts and stylolites (filled by bitumen). Intergranular and shelter porosities filled by allomicrite and blocky calcite cement. Microcrystalline quartz, megaquartz and chalcedony due to silicification of brachiopod shells, crinoid ossicles and matrix. Fissures filled by blocky calcite cement and bitumen	Low- to moderate-energy, middle-ramp environment, with current patterns altered by Ricklow mud mound complex vestigial topography (cf. Nolan et al. 2017)	Post mud mound complex facies

Abundances in volume percentage: Abundant—A (> 50%); very common—VC (50–30%); common—C (30–10%); sparse—S (10–5%); rare—R (5–2%); very rare—VR (> 2%) following Flügel (2004)

Table 2 Lithofacies associations forming the mud mound complex of Ricklow Quarry

Lithofacies association	Description	Stratigraphic position	Thickness	Lateral extent
Lithofacies Association 1 (LA1)—mud mound complex basal unit	Nodular, irregular beds (3–5 cm thick) of brachiopod bryozoan packstone/rudstone with patches of automicrite boundstone (L2), irregularly interbedded and laterally transitional to more sparsely fossiliferous 5–8 cm thick beds of automicrite boundstone (L3) and thicker, up to 100 cm, lenses of brachiopod bryozoan wackestone/floatstone (L4) Brachiopod shells articulation ratio: 37.8%	Occurring over beds of L1. Laterally equivalent to beds of L5. Overlain by LA2	10 m	?100 m
Lithofacies Association 2 (LA2)—mud mound complex core	Lens-shaped convex-up units with a thickness of 1–2 m and a diameter of 4–5 m, consisting of mm- to dm-size patches of clotted peloidal micrite boundstone (L7) and minor fenestellid bryozoan boundstone/cementstone (L6), with mm- to dm-size patches of skeletal grainstone/rudstone in-between (L8). Areas (dm- to m-size) consisting of automicrite boundstone with skeletal packstone/rudstone patches show poorly defined, irregular, 5–15 cm thick beds (L9). Radiaxial fibrous calcite cement is widespread in cavities sustained by automicrite and bryozoan fronds. Alveolar structures, non-luminescent brownish pendant calcite cement, isopachous fine reddish equant calcite cement and non-luminescent dogtooth to equant calcite cements are abundant near the top Brachiopod fauna articulation ratio: 56.8%	Occurring above LA1 and L5 beds. Laterally equivalent to LA3 and L12 in off-mud mound complex areas. Onlapped by L13, L14, L15	10 m	250 m
Lithofacies Association 3 (LA3)—mud mound complex flank beds	Poorly to well-bedded inclined (up to 44°) beds with a thickness of 10–100 cm consisting nearer to the mud mound complex core of a leiolite boundstone mixed with burrowed skeletal wackestone/floatstone (L10), further away downslope of skeletal packstone–rudstone (L11) Brachiopod fauna articulation ratio: 38.0%	Occurring above LA1 and L5 beds. Forming the lateral transition zone between LA2 and L12 beds. Overlain by lithofacies L13, L14, L15	8 m	Wedge around mud mound complex core, 10–30 m wide

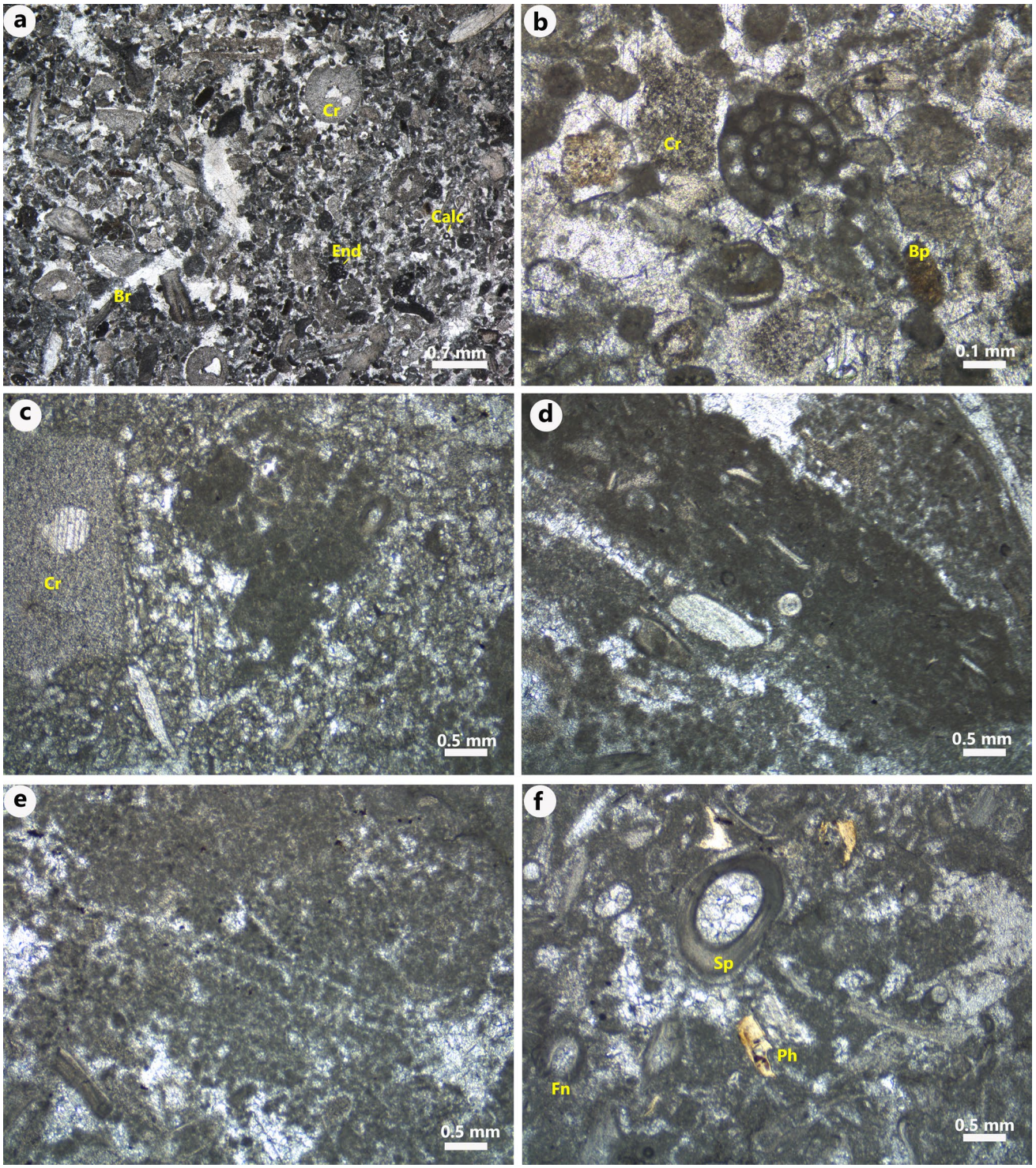

Fig. 6 Lithofacies underlying the mud mound complex (pre-mound) and forming the complex basal unit (Lithofacies Association 1—LA1). **a** Photomicrograph of Lithofacies L1: peloidal–skeletal packstone to grainstone, with crinoid ossicles (Cr), brachiopod shells (Br), micritised endothyrid foraminifers (End), and calcispheres (Calc). **b** Photomicrograph of L1 showing detail of endothyrid, with fragmented crinoid ossicles (Cr) and "black pebbles" (Bp). **c** Photomicrograph of Lithofacies L2: brachiopod bryozoan packstone/rudstone. Detail of clotted peloidal micrite intraclast and crinoid ossicle (Cr) in allomicrite matrix partially re-crystallised in microsparite. **d** Photomicrograph of L2 showing clotted peloidal micrite nodule with abundant calcified siliceous sponge spicules, into a clotted peloidal micrite patch. **e** Photomicrograph of Lithofacies L3: automicrite boundstone showing detail of clotted peloidal micrite. **f** Photomicrograph of L3 showing brachiopod spines (Sp), fenestellid bryozoan frond debris (Fn), and phosphatic grains (Ph) into clotted peloidal micrite

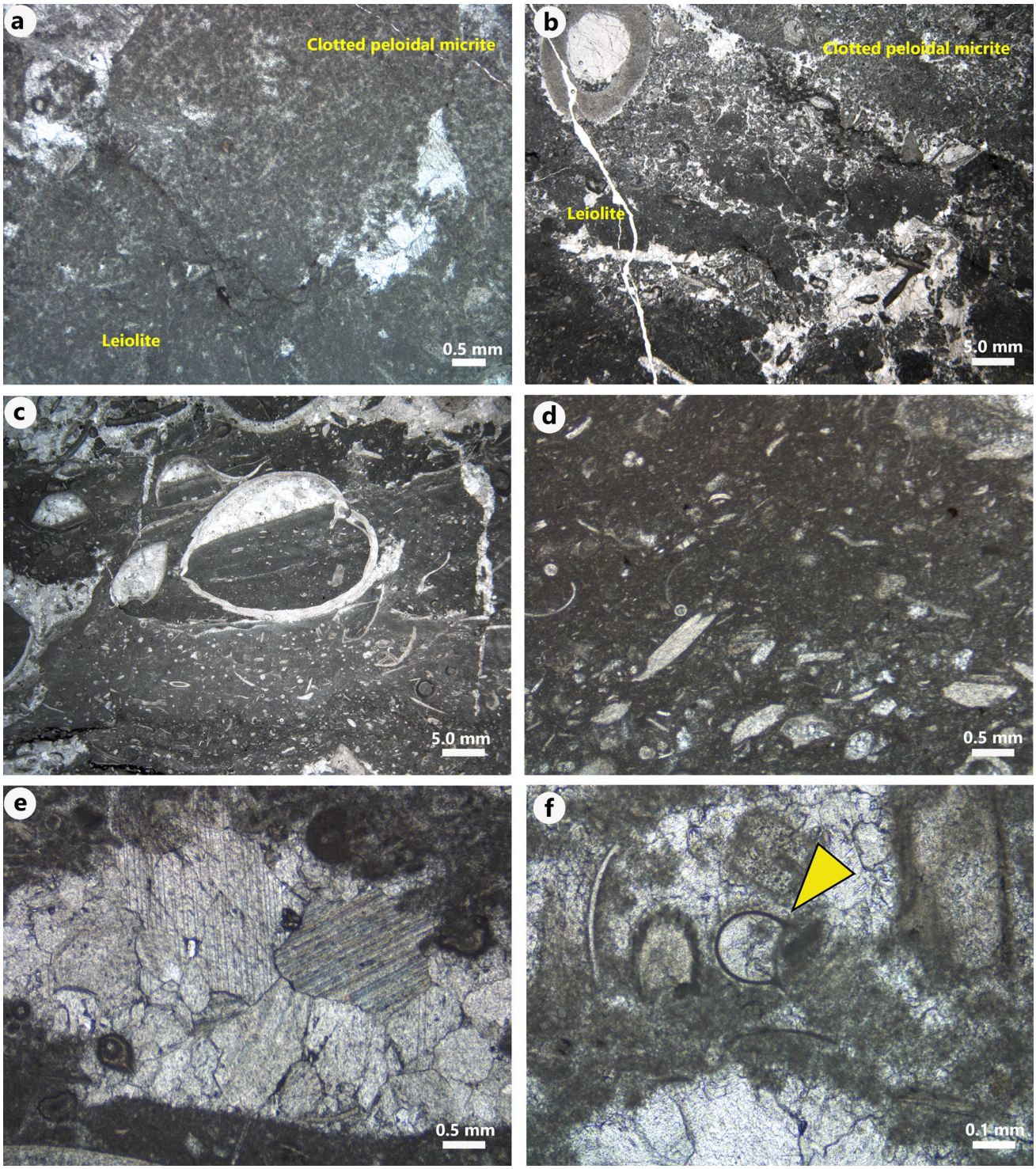

Fig. 7 Lithofacies in the mud mound complex basal unit (Lithofacies Association 1—LA1). **a** Photomicrograph of Lithofacies L3: automicrite boundstone. Detail of leiolite passing to clotted peloidal micrite sustaining a primary cavity filled by blocky calcite cement (on the right). **b** Photomicrograph of L3, showing leiolite micrite portions alternating with clotted peloidal micrite. **c** Photomicrograph of Lithofacies L4: brachiopod bryozoan wackestone/floatstone. Note the abundance of articulated brachiopod shells and skeletal debris roughly isoriented in allomicrite. **d** Photomicrograph of L4 showing detail of skeletal debris in allomicrite matrix. **e** A stromatactis-like cavity in L4 filled by blocky calcite cement within a leiolite micrite boundstone patch. **f** Photomicrograph of L4 showing a *Tuberitina* foraminifer encrusting clotted peloidal micrite

Table 3 Brachiopod faunal list for the three units of the Ricklow mud mound complex: mud mound complex basal unit (Lithofacies Association 1); mud mound complex core (Lithofacies Association 2); mud mound complex flank beds (Lithofacies Association 3)

Mud mound complex basal unit (LA1)	Mud mound complex core (LA2)	Flank beds (LA3)
Productida	**Productida**	**Productida**
Alitaria aff. *triquetra* (Muir-Wood, 1928)	*Alitaria* aff. *triquetra* (Muir-Wood, 1928)	*Quasiavonia aculeata* (Sowerby, 1814)
Quasiavonia aculeata (Sowerby, 1814)	*Overtonia fimbriata* (Sowerby, 1824)	*Breileenia radiata* Brunton, in Brunton and Lazarev 1997
?*Quasiavonia* sp.	*Avonia* sp.	*Antiquatonia hindi* (Muir-Wood, 1928)
Krotovia spinulosa (Sowerby, 1814)	*Quasiavonia aculeata* (Sowerby, 1814)	*Antiquatonia insculpta* (Muir-Wood, 1928)
Carringtonia cf. *carringtoniana* (Davidson, 1862)	*Krotovia spinulosa* (Sowerby, 1814)	*Dictyoclostus pinguis* (Muir-Wood, 1928)
Limbifera sp.	*Breileenia radiata* Brunton, in Brunton and Lazarev 1997	*Buxtonia scabricula* (Sowerby, 1814)
Productus sp.	*Geniculifera keyserlingiana* (de Koninck, 1843)	*Echinoconchus punctatus* (Sowerby, 1822)
Eomarginifera cf. *laqueata* (Muir-Wood, 1928)	*Productus* cf. *productus* (Martin, 1809)	
Antiquatonia hindi (Muir-Wood, 1928)	*Eomarginifera* cf. *laqueata* (Muir-Wood, 1928)	
Antiquatonia aff. *hindi* (Muir-Wood, 1928)	*Antiquatonia hindi* (Muir-Wood, 1928)	
Antiquatonia insculpta (Muir-Wood, 1928)	*Antiquatonia* aff. *hindi* (Muir-Wood, 1928)	
Dictyoclostus pinguis (Muir-Wood, 1928)	*Antiquatonia insculpta* (Muir-Wood, 1928)	
Pugilis cf. *kilbridensis* (Muir-Wood, 1928)	*Dictyoclostus pinguis* (Muir-Wood, 1928)	
Pugilis cf. *scotica* (Sowerby, 1814)	*Pugilis* cf. *kilbridensis* (Muir-Wood, 1928)	
Buxtonia scabricula (Sowerby, 1814)	*Buxtonia scabricula* (Sowerby, 1814)	
Buxtonia sp.	Buxtoniinae gen. et sp. indet.	
Echinoconchus punctatus (Sowerby, 1822)	*Echinoconchus punctatus* (Sowerby, 1822)	
Pustula cf. *pustulosa* (Phillips, 1836)	*Pustula* cf. *pustulosa* (Phillips, 1836)	
Linoprotonia sp.	*Linoprotonia* sp.	
Orthotetida	**Orthotetida**	**Orthotetida**
–	*Schellwienella* sp.	Orthotetida gen. et sp. indet.
	?*Serratocrista* aff. *dalriensis* McIntosh, 1974	
Orthida	**Orthida**	**Orthida**
Schizophoria resupinata (Martin, 1809)	*Scizophoria resupinata* (Martin, 1809)	*Schizophoria resupinata* (Martin, 1809)
Schizophoria cf. *connivens* (Phillips, 1836)		*Schizophoria* cf. *connivens* (Phillips, 1836)
Rhynchonellida	**Rhynchonellida**	**Rhynchonellida**
Pleuropugnoides pleurodon (Phillips, 1836)	*Pleuropugnoides pleurodon* (Phillips, 1836)	*Pleuropugnoides pleurodon* (Phillips, 1836)
Propriopugnus pugnus (Martin, 1809)	*Propriopugnus pugnus* (Martin, 1809)	*Propriopugnus pugnus* (Martin, 1809)
Spiriferida	**Spiriferida**	**Spiriferida**
Martiniinae gen. et sp. indet.	*Crurithyris urei* (Fleming, 1828)	*Latibrachythyris rotundata* (Sowerby, 1825)
Latibrachythyris cf. *crassa* (de Koninck, 1843)	?*Fusella* sp.	
Latibrachythyris rotundata (Sowerby, 1825)	*Latibrachythyris* cf. *crassa* (de Koninck, 1843)	
Phricodothyris paricosta George, 1932	*Latibrachythyris rotundata* (Sowerby, 1825)	
Phricodothyris cf. *periculosa* George, 1932	Brachythyrididae gen. et sp. indet.	
	?*Reticularia* cf. *mesoloba* (Phillips, 1836)	
	Phricodothyris paricosta George, 1932	
	Phricodothyris cf. *periculosa* George, 1932	
Spiriferinida	**Spiriferinida**	**Spiriferinida**
–	?*Punctospirifer* sp.	–
Terebratulida	**Terebratulida**	**Terebratulida**
Harttella oakleyi Brunton, 1982	*Harttella oakleyi* Brunton, 1982	Terebratulida gen. et sp. indet.
?*Balanoconcha* sp.	*Beecheria* sp.	
	?*Balanoconcha* sp.	

Systematic description and discussion of the fauna from the Ricklow mud mound complex was provided by Carniti et al. (2022)

fossiliferous lithofacies. These lenses have an irregular morphology, with poorly defined base and edges in relation to the surrounding less-fossiliferous lithofacies. A few lenses have a sharp basal surface with abundant productides in life position, overlain by articulated millimetre-size terebratulides, spiriferides, rhynchonellides, along with other productides. Brachiopod concentration does not vary vertically in the mud mound complex core. A faunal list of brachiopod species for unit LA2 is given in Table 3.

The LA2 mud mound complex core passes laterally to a massive to poorly bedded leiolite boundstone (L10), and further away from the core to 10–50 cm thick, inclined beds (dipping up to 44° with respect to the inferred adjacent horizontal sea-floor) constituted by skeletal packstone/rudstone (L11; Figs. 3b, 5e), forming a 8 m thick,

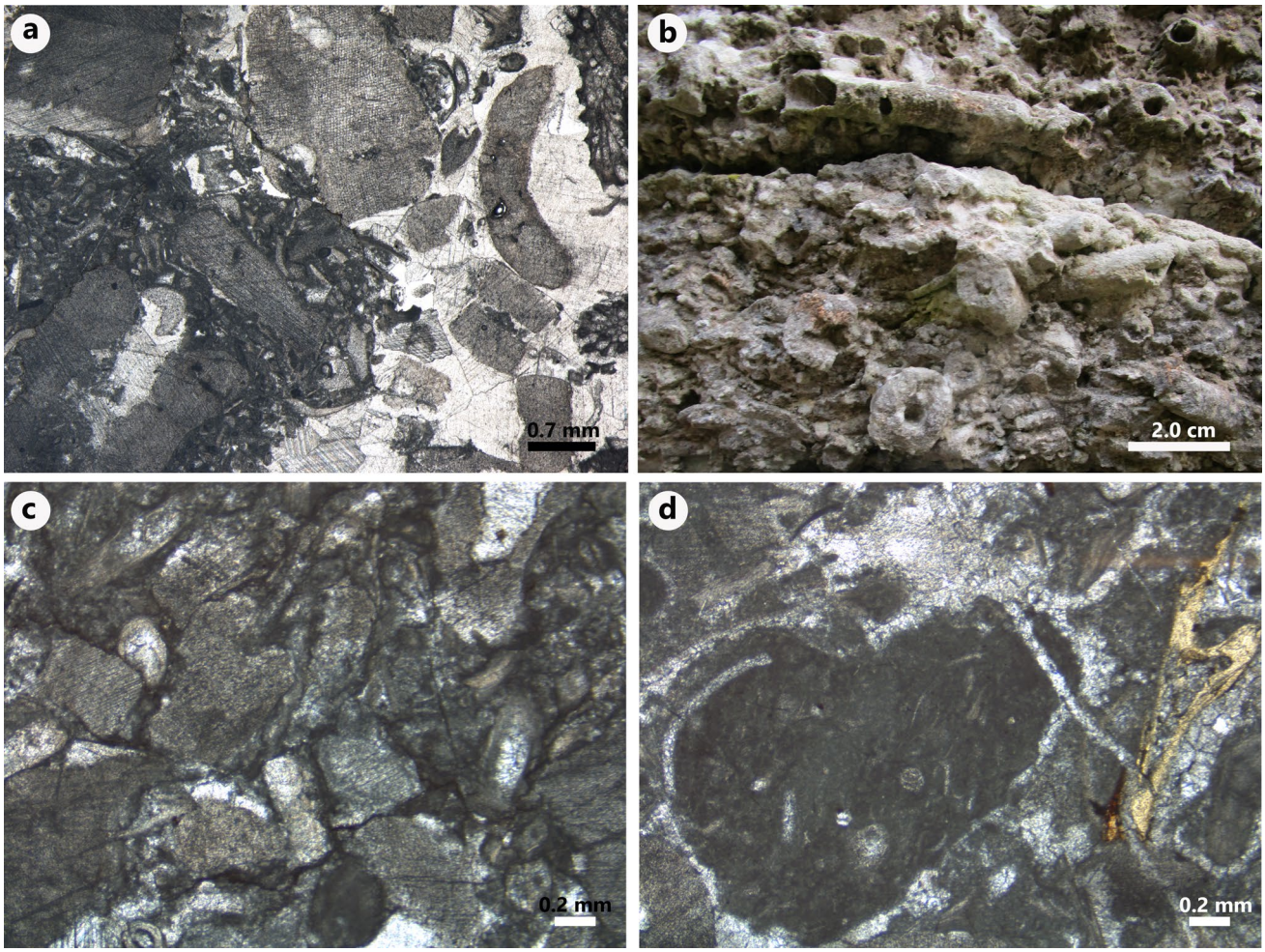

Fig. 8 Lithofacies lateral to the mud mound complex. **a** Photomicrograph of Lithofacies L5: crinoidal grainstone/rudstone with automicrite patches. **b** Outcrop photograph of L5. **c** Photomicrograph of Lithofacies L12: crinoidal packstone/rudstone. Note compacted fitted texture with sutured grain contacts in an area dominated by crinoid ossicles. **d** Photomicrograph of L12 showing leiolite intraclast and phosphatic grain (likely fish scale; on the right)

10–30 m wide wedge around the mud mound complex. L10 is dominated by leiolite with few skeletal grains and millimetre-size cavities filled by blocky calcite cement, while 30–40% of the rock volume consists of patches of burrowed skeletal wackestone/floatstone with roughly isoriented sparse brachiopods, sponge spicules, bryozoans, crinoids, and clotted peloidal micrite intraclasts (Fig. 11a–d). L11 is a brachiopod–bryozoan–crinoid–ostracod packstone/rudstone with sparse bivalves, sponge spicules, and automicrite intraclasts (Fig. 11e, f). The association of L10 and L11 forms the mud mound complex flank beds which are labelled as Lithofacies Association 3 (LA3). Flank beds dip out from the mud mound complex core; the variety of dip values of flank beds reveals the former presence of multiple mud mounds laterally accreting to build the mud mound complex (Fig. 3b). In the flank beds, most brachiopods occur articulated but not in life position (articulation ratio 38.0%); the fauna is apparently less diversified than in LA1 and LA2 (Table 3). LA3 passes laterally to crinoidal packstone/rudstone (L12; Fig. 3b). L12 is similar to L5 but the packstone texture is dominant (Fig. 8c) with millimetre-size skeletal wackestone patches, whereas automicrite forms only intraclasts (Fig. 8d).

Dissolution vugs, rhizolith, alveolar texture, Fe oxide red colour staining of grains and cement occur at the top of the mud mound complex (Figs. 5, 12a, b). Crinoidal grainstone/rudstone beds (L13), 5–40 cm thick, with sparse brachiopods and rare angular intraclasts of clotted peloidal micrite boundstone (Fig. 12c, d), onlap the flank of the mud mound complex (Fig. 3b) and are characterised by the common occurrence of pendant calcite cements (Fig. 12c).

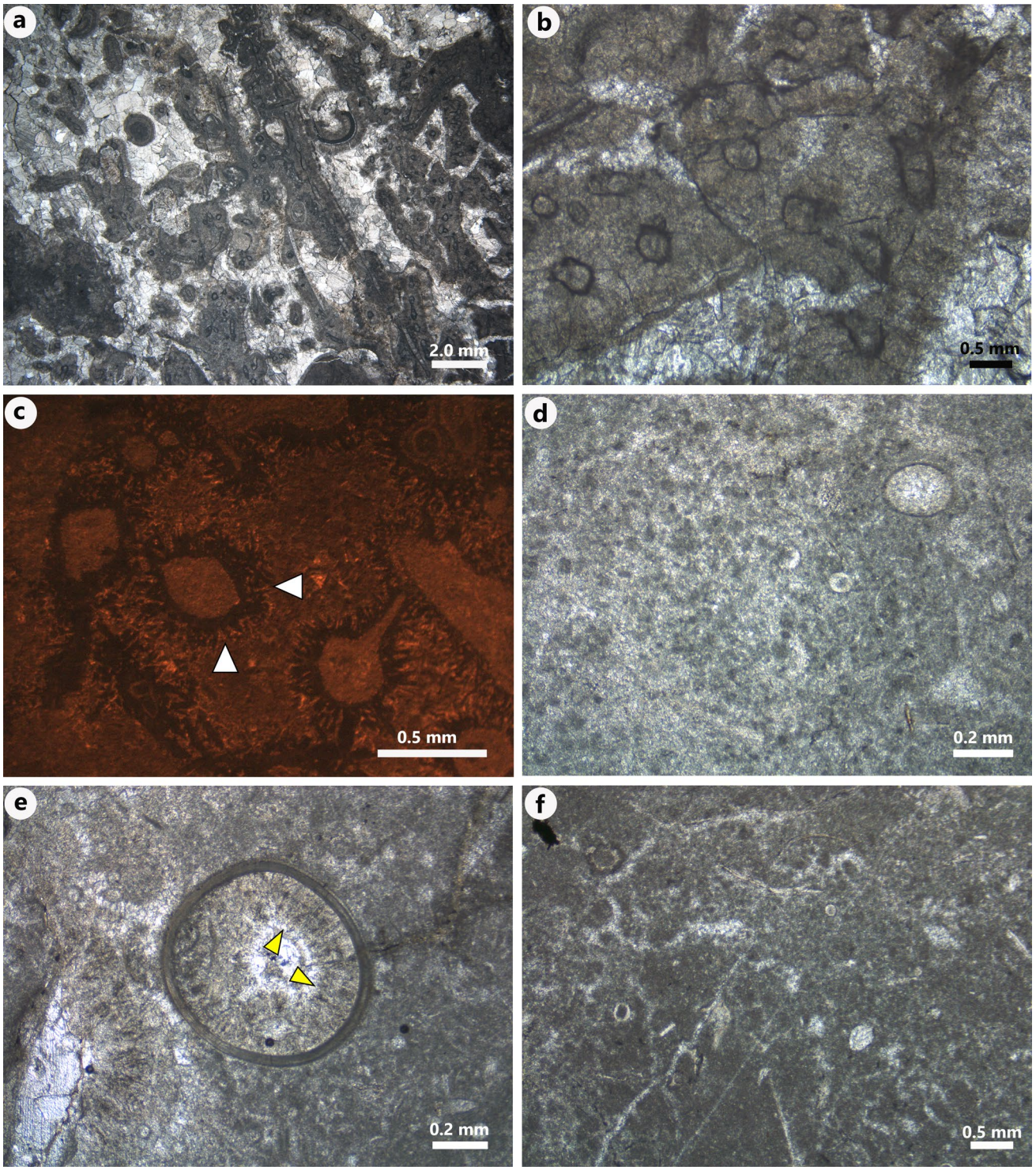

Fig. 9 Lithofacies in the mud mound complex core (Lithofacies Association 2—LA2). **a** Photomicrograph of Lithofacies L6: fenestellid bryozoan boundstone/cementstone. Note abundant radiaxial fibrous calcite cement around fenestellid fronds; framework cavities are also filled by blocky calcite cement. **b** Photomicrograph of L6, showing detail of fenestellid fronds with isopachous radiaxial fibrous calcite cement. **c** Cathodoluminescence photomicrograph of L6 showing non-luminescent isopachous radiaxial fibrous calcite cement (arrows) around luminescent re-crystallised fenestellid fronds. Framework cavities are also filled by luminescent blocky calcite cement. **d** Photomicrograph of Lithofacies L7: clotted peloidal micrite boundstone. Detail of peloids within microsparite (more closely packed on the right). **e** Photomicrograph of L7, showing a productide spine filled by radiaxial fibrous calcite cement, embedded within clotted peloidal micrite. **f** Photomicrograph of L7, showing detail of closely packed peloids and minor leiolite patches sustaining 500 µm wide primary cavities

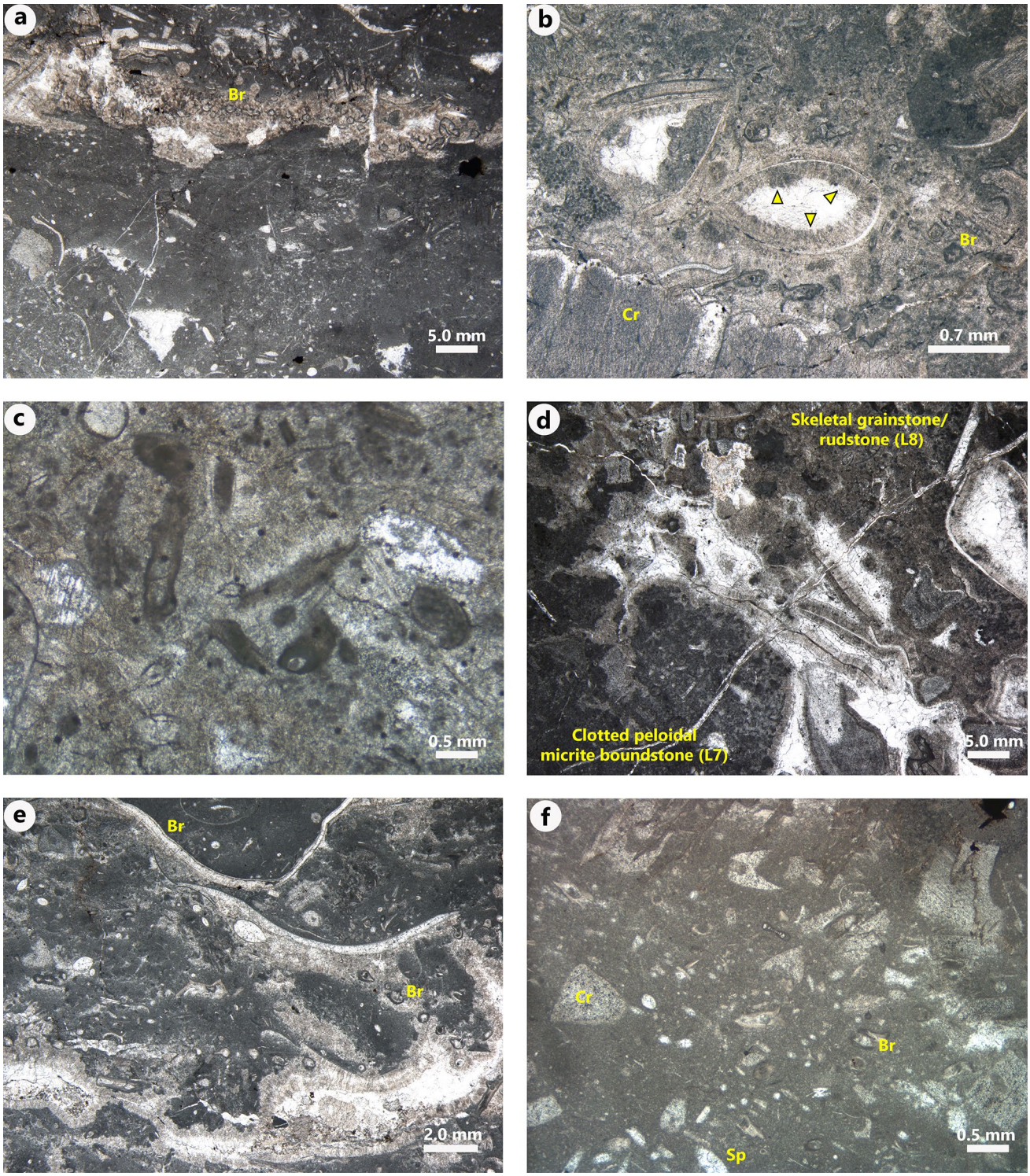

Fig. 10 Lithofacies in the mud mound complex core (Lithofacies Association 2). **a** Photomicrograph of Lithofacies L7: clotted peloidal boundstone, showing clotted peloidal micrite boundstone patches alternated with volumes filled by bryozoan frond fragments (Br) and radiaxial fibrous calcite cement (L8). **b** Photomicrograph of Lithofacies L8: skeletal grainstone/rudstone, with articulated brachiopod shells surrounded and filled by isopachous radiaxial fibrous calcite cement (arrows), crinoids (Cr), and fenestellid bryozoan debris (Br). **c** Photomicrograph of L8, showing detail of fenestellid bryozoan frond debris surrounded by microsparite with sparse peloids and radiaxial fibrous calcite cement. **d** Photomicrograph showing the irregular boundary between L7 and L8. **e** Photomicrograph of Lithofacies L9: automicrite boundstone with skeletal packstone/rudstone patches. Note the high skeletal content, 1–5 mm wide primary cavities filled by radiaxial fibrous calcite cement and fenestellid bryozoan frond fragments (Br), and minor wackestone patches (above). **f** Photomicrograph of L9, showing detail of wackestone patch with skeletal debris: crinoids (Cr), sponge spicules (Sp), bryozoans (Br)

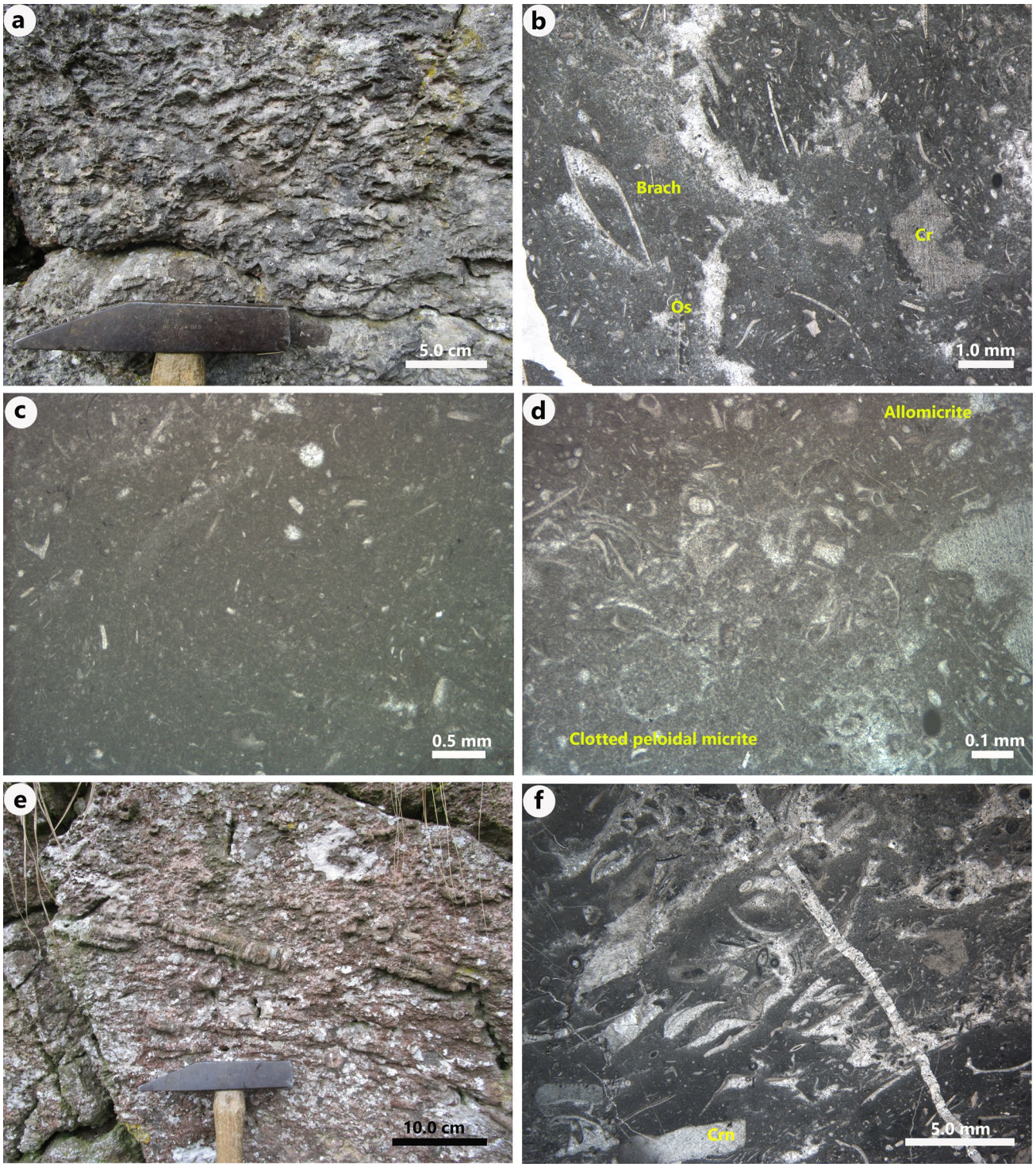

Fig. 11 Lithofacies in the mud mound complex flank beds (Lithofacies Association 3—LA3). **a** Outcrop photograph of Lithofacies L10: leiolite boundstone. Few skeletal grains (mainly brachiopod shells) protrude out of the weathered rock surface. **b** Photomicrograph of L10, showing burrowed skeletal wackestone with ostracod (Os), brachiopods (Brach), and crinoids (Cr). **c** Photomicrograph of L10, showing burrowed skeletal wackestone with a few skeletal debris. **d** Photomicrograph of L10, showing the transition from densely packed clotted peloidal micrite with few skeletal debris to allomicrite with abundant skeletal fragments. **e** Outcrop photograph of Lithofacies L11: skeletal packstone/rudstone, with common isoriented crinoid stems. **f** Photomicrograph of L11, showing isoriented disarticulated brachiopod shells sheltering primary cavities in the allomicrite matrix, along with crinoid ossicles (Crn) and bryozoan debris

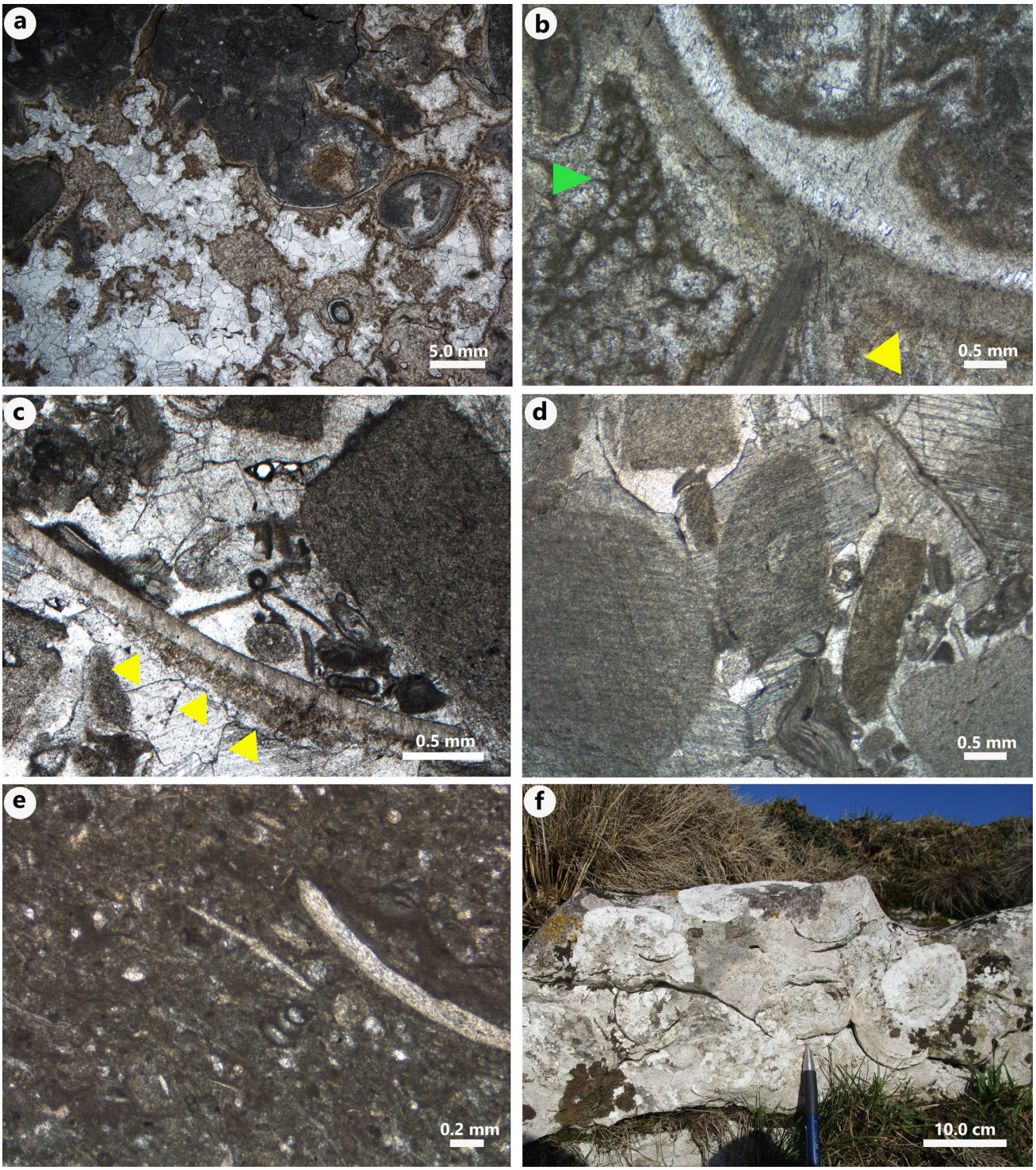

Fig. 12 Lithofacies at the top and overlying the mud mound complex. **a** Photomicrograph of Lithofacies L7 (LA2) showing irregular dissolution vugs filled by non-luminescent reddish fine-grained equant calcite cement and luminescent coarse-grained blocky calcite cement. **b** Photomicrograph of Lithofacies L8 (LA2) showing alveolar structures (green arrow, on the left) and brownish pendant cement (yellow arrow, on the lower right). **c.** Photomicrograph of Lithofacies L13: crinoidal grainstone/rudstone. Detail of brachiopod valve with brownish pendant calcite cement (arrows). **d** Photomicrograph of Lithofacies L13 showing crinoid ossicles and brachiopod shell fragments (below) with intergranular porosity filled by syntaxial and blocky calcite cements. **e** Photomicrograph of Lithofacies L14: molluscan wackestone to packstone. Note bivalve shells and foraminifers isoriented within the allomicrite matrix. **f** Outcrop photograph of Lithofacies L15: gigantoproductins packstone/rudstone

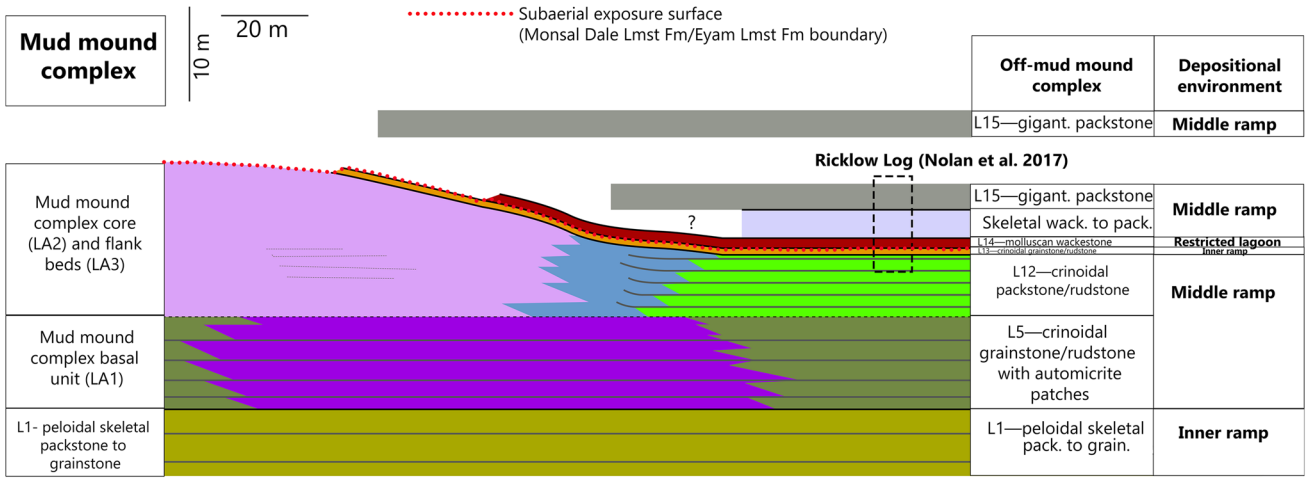

Fig. 13 Lithofacies scheme and depositional model for the mud mound complex and off-mud mound complex area. For a description of lithofacies L1–L15 see Table 1; for a description of lithofacies associations LA1–LA3 see Table 2; for a description of lithofacies in the Ricklow Log refer to Nolan et al. (2017)

L13 is overlain by 50 cm thick beds of molluscan wackestone to packstone (L14), with disarticulated and fragmented common bivalves, sparse sponge spicules, and brachiopods (Fig. 12e). Above, there are two metre-scale beds of packstone/rudstone (L15), dominated by shells in life position of several species of the genus *Gigantoproductus*, alongside sparse crinoids and peloids (Fig. 12f). Also L14 and L15 onlap the mud mound complex (Figs. 3b, 5a).

Interpretation of depositional environments

Figure 13 shows a summary of the lithofacies architecture and depositional model of the mud mound complex of Ricklow Quarry and the units underlying and overlying the buildup. Also, it provides a lithofacies correlation scheme between the mud mound complex and the log to the east of it described by Nolan et al. (2017, Ricklow Log; Fig. 3b).

Peloidal–skeletal packstone to grainstone (L1) was deposited before the onset of the mud mound complex in a moderate-energy, subtidal, open-marine inner-ramp setting, as suggested by the abundance of peloids, bioclasts, and endothyrid foraminifers (Gallagher 1988; Della Porta et al. 2005). Dark-coloured lithoclasts are interpreted as "black pebbles": pedogenised material reworked in the transgressive strata following subaerial exposures (Flügel 2004).

The overlying mud mound complex basal LA1 (L2, L3, L4) represents the initiation of a microbial-metazoan (bryozoans, siliceous sponges, brachiopods) community on the sea-floor, leading to the production of automicrite, in a moderate-energy middle-ramp environment. This depositional setting reconstruction is based on the absence of sedimentary structure evidence of wave action and a faunal assemblage with bryozoans, crinoids, and few trochospiral (*Tetrataxis*) and encrusting (*Tuberitina*) foraminifer morphologies, associated with Gallagher and Somerville's (2003) Biofacies 1: marine low-energy setting with a depth of more than 20 m, below fair-weather wave base. Also, siliceous sponges, whose presence is evidenced by common calcite-replaced spicules and nodules of early lithified automicrite embedding isoriented sponge spicules, representing calcified sponge bodies (Fig. 6d; cf. tuberoids, Fritz 1958, Warnke 1995), are indicative of subtidal low-energy environments (Wilkinson and Trott 1985; Brunton and Dixon 1994; Cózar et al. 2019a). Hydrodynamic energy was, however, sufficient to sustain the suspension feeders and rework carbonate mud, resulting in the abundance of allomicrite in LA1, and to prevent vertical aggradation of automicrite boundstone beds. A moderate-energy setting is further supported by the low articulation ratio of brachiopods. Carniti et al. (2022) proposed moderate-energy, mesotrophic environment for LA1, based on the dominance in terms of biovolume of both large-sized spiriferides (specimens of species of *Latibrachythyris* up to 50 mm wide) and large-sized productides (e.g. *Echinoconchus punctatus* Sowerby, 1822) characterised by specimens up to 51 mm wide) in the Ricklow mud mound complex. Spiriferides had a complex feeding mechanism consisting of a spirolophe lophophore. According to Pérez-Huerta and Sheldon (2006), they were able to generate strong unidirectional inhalant currents allowing them to attain a large size in environments with high food supply (e.g. Angiolini 2007). The feeding mechanism of productides consisted of cilia attached to the dorsal valve interior and they were, thus, able to generate

multi-directional currents and take food resources from a larger area around the shell, reaching a large size mostly in environments with few and dispersed food resources (Pérez-Huerta and Sheldon 2006).

Crinoidal grainstone/rudstone beds (L5) adjacent to LA1 were deposited in the same moderate-energy environment in areas dominated by crinoid communities, as indicated by the low amount of allomicrite and isorientation of unfragmented crinoid ossicles and stems.

The overlying mud mound complex core (LA2: L6, L7, L8, L9) and flank beds (LA3: L10, L11) were deposited in a similar subtidal middle-ramp environment, but with lower-energy than LA1. Decrease of hydrodynamic energy between the deposition of LA1 and that of LA2 and LA3 is supported by the presence in LA2 of metre-scale lens-shaped automicrite units (L6, L7, L8), different from the tabular units of LA1. Lens-shaped units formed through lateral and vertical accretion decametre-scale lens-shaped mud mounds, associated to form a mud mound complex with some metre-relief over the sea-floor. Buildup relief during deposition is supported by the dip of the flank beds with respect to present-day-horizontal, up to 44°; as the regional dip is near to horizontal (Aitkenhead et al. 1985), flank beds dip is roughly close to the depositional dip with respect to the horizontal sea-floor. Onlap of the mud mound complex by the overlying beds (cf. Della Porta et al. 2002) strengthens this interpretation.

Decrease in hydrodynamic energy between the deposition of LA1 and LA2 is also supported by less allomicrite in LA2 than in the basal unit LA1. Furthermore, Carniti et al. (2022) suggested a decrease in hydrodynamic energy and thus food distribution during deposition of LA2 with respect to LA1, based on the dominance of productide brachiopods in terms of biovolume.

The flank beds are adjacent to crinoidal packstone/rudstone beds (L12). L12 shows the same texture, composition, and stratigraphic position of the peloidal intraclastic packstone beds with crinoids, bryozoans, ostracods, and brachiopods described in the basal 2 m thick part of the Ricklow Log by Nolan et al. (2017). Calcareous algae are absent from the mud mound complex core and little reworked debris is found in L12 (Nolan et al. 2017), indicating a dysphotic setting.

The mud mound complex in Ricklow, thus, developed in a middle-ramp, dysphotic environment with dispersed food resources, with low to moderate hydrodynamic energy level.

Crinoidal grainstone/rudstone (L13) beds onlapping the mud mound complex were deposited in a high-energy inner-ramp setting (Fig. 13). Good sorting, abundance of endolith microborings, and absence of allomicrite corroborate this interpretation. A cross-bedded 0.5 m thick lens of the same lithofacies occur in the Ricklow Log (Nolan et al. 2017) overlying the middle-ramp crinoidal packstone beds (L12; Fig. 13), and was interpreted by Nolan et al. (2017) as a subaqueous dune. Relative sea-level fall led to the demise of the mud mound complex growth; the partially to fully lithified buildup then provided the automicrite intraclasts in L13 (Fig. 13).

Widespread occurrence of pendant cements and other diagenetic features interpreted as due to vadose and phreatic meteoric diagenesis at the top of the mud mound complex core (LA2), in L13 both near the mud mound complex and in the Ricklow Log (Nolan et al. 2017), and minor occurrence of these features into LA1 and the lower portion of LA2 (Table 1), suggest that relative sea-level fall led to subaerial exposure of the study area after deposition of L13 (Figs. 5, 13).

After subaerial exposure, the molluscan wackestone to packstone (L14) was deposited in restricted lagoon environments with low-energy and variable salinity in-between the mud mound complexes of the intraplatform ramp (cf. Della Porta et al. 2002). This is indicated by the abundance of allomicrite and molluscs and the absence of stenohaline echinoderms and bryozoans (Nolan et al. 2017). After a stratigraphic gap, beds of the gigantoproductins packstone/rudstone (L15) occur onlapping the mud mound complex. These were deposited in a low-energy, middle-ramp environment, as indicated by the absence of wave reworking and the presence of allomicrite. Both L14 and L15 are described in the Ricklow Log (Nolan et al. 2017; Angiolini et al. 2019) separated by a middle-ramp skeletal wackestone to packstone with brachiopods, ostracods, and crinoids (Fig. 13; Nolan et al. 2017).

Discussion

Initiation of the mud mound complex

The Ricklow Quarry mud mound complex deposition initiated during accommodation creation. This is a common feature of several Palaeozoic mud mounds (cf. Pickard 1992; Keupp et al. 1993; Aretz et al. 2012; Cózar et al. 2019a; Zhou and Pratt 2019; Yao and Aretz 2020). Rapid accommodation creation decreases sedimentation rate, thus resulting in firmground formation: these two conditions are suitable for sea-floor colonisation by a suspension feeder benthic community consisting of bryozoans, brachiopods, and siliceous sponges.

The metazoan community was probably associated with microbial mats, whose presence can be inferred from the mud textures indicative of microbially mediated in-situ precipitation (cf. Lees and Miller 1995; Monty 1995; Pratt 1995; Pickard 1996). Microbial communities were probably not forming widespread mats covering the sea-floor:

otherwise, the presence of widespread microbial mats would have resulted in laminated automicrite deposits with few skeletal remains, e.g. stromatolite, as seen in modern hypersaline lakes (e.g. Dupraz et al. 2004). No evidence of stromatolite was found in any lithofacies association forming the Ricklow Quarry mud mound complex. It is likely that competition for space with the rich sessile metazoan community colonising the sea-floor and limited grazing activity of gastropods and trilobites, whose rare remains occur in thin sections, prevented widespread microbial mats formation. Instead, siliceous sponges likely hosted abundant and diverse microbial communities in the mesohyl (cf. Brunton and Dixon 1994), as is the case for modern demosponges (Vacelet and Donadey 1977; Wilkinson 1978a, 1978b; Wilkinson et al. 1984; Reitner 1993; Tout et al. 2017). Also, decaying sponge tissues, as well as other metazoan tissues in the sediment, provided suitable organic substrates for microbial mats, leading to the initiation of microbially mediated mineralisation processes (cf. McConnaughey 1989; Frankel and Bazylinski 2003; Weiner and Dove 2003; Guido et al. 2013, 2022; Lee and Riding 2020) and/or passive organomineralisation of sponge soft tissues (cf. Reitner 1993; Reitner et al. 1995a, 1995b; Warnke 1995; Neuweiler and Burdige 2005; Neuweiler et al. 2007; Shen and Neuweiler 2018).

These processes led to the deposition of the tabular automicrite units of LA1, and later to the lens-shaped units of LA2. Bryozoans and brachiopods were not forming a skeletal framework, but their skeletons associated with the mineralised sponge bodies and automicrite formed an irregular stiff surface with up-right growth forms and depressions.

Mud mounds developed in various localities in the Derbyshire Carbonate Platform at the same stratigraphical level as the Ricklow Quarry mud mound complex, at the top of the Monsal Dale Limestone Fm (Gutteridge 1995). A literature review of the lithofacies distribution in the upper Monsal Dale Limestone Fm (e.g. Aitkenhead et al. 1985; Gutteridge 1989a; Harwood 2005) showed that the mud mounds developed aligned along the north-eastern margin of the platform, near the southern platform margin and in intraplatform inner–outer-ramp settings (Fig. 14).

The event of creation of accommodation leading to the initiation of the Ricklow mud mound complex might have been the trigger for growth of all mud mounds at the top of the Monsal Dale Limestone Fm, either related to upper Visean reactivation of extensional tectonics to the north of the Wales-Brabant High in northern England (Gawthorpe et al. 1989), and/or to eustatic sea-level rise. Mississippian sedimentation was governed by global sea-level changes, resulting in third-order sequences which might be synchronous worldwide (e.g. Ross and Ross 1985; Herbig 2016). Third-order sequence boundaries occurring in the lower and middle Brigantian (upper Visean) of Germany, Belgium and southwestern England (Herbig 2016 and references therein), might be coeval with the boundaries between D5b, D6a, and D6b transgressive–regressive cycles of Ramsbottom (1973, 1977) in northern England. These cycle boundaries seem coeval with the upper boundaries of the Bee Low Limestone Fm and the Monsal Dale Limestone Fm, corresponding to regional subaerial exposure surfaces. The latest Visean was also a time of high-frequency fourth and fifth order glacioeustatic fluctuations (Horbury 1989; Smith and Read 2000; Wright and Vanstone 2001), with an inferred amplitude of 40–100 m (Rygel et al. 2008), followed by the initiation of the Serpukhovian–middle Bashkirian glacial period (C_2) of the Late Palaeozoic Ice Age (Isbell et al. 2003; Fielding et al. 2008).

More data on the lithofacies underlying the mud mounds in the Monsal Dale Limestone Fm are necessary to clarify the role of glacioeustacy and local tectonics on the initiation of Derbyshire upper Visean mud mounds.

Mud mound complex growth: development of relief

A marked change in automicrite texture is observed between the basal LA1 unit and the LA2 mud mound complex core. While in LA1 automicrite beds (L3) have few primary cavities and microsparite content, automicrite in LA2 (L7, L9) is microsparite-rich and forms millimetre to decimetre-size patches with abundant radiaxial fibrous calcite cement and skeletal grains in-between (L8).

Greater accommodation and lower hydrodynamic energy during deposition of LA2 in comparison with LA1 allowed the mud mound complex core to grow both horizontally and vertically and to develop a convex-upward structure sustained by automicrite associated with bryozoans, brachiopods, and siliceous sponges. Automicrite precipitation led to early lithification of the mud mound complex core and then further vertical growth, resulting in metre-scale relief development over the sea-floor. Topographic relief over the sea-floor allowed water pumping by currents into the system of primary cavities in the mud mound complex core leading to the precipitation of radiaxial fibrous calcite cement (cf. Kendall 1985).

Bryozoan dominated areas resulted in deposition of the fenestellid bryozoan boundstone/cementstone lithofacies (L6); scarcity of automicrite in L6 is likely linked to scarcity of siliceous sponges. Other sponge-poor areas were the ones dominated by fenestellid bryozoans and brachiopods: absence of sponges led to little automicrite formation, leading to no vertical accretion, mud reworking and bryozoan fragmentation. These areas resulted in the deposition of the poorly bedded automicrite boundstone with skeletal packstone/rudstone patches (L9).

Brachiopod distribution

This study demonstrates that brachiopods are common skeletal components in all lithofacies of the mud mound complex at Ricklow, even in the automicrite-rich ones (L7, L9). The centimetre- to decimetre-size lenses of L8 with a richer brachiopod content in the mud mound complex core (LA2) might correspond to those interpreted by Gutteridge (1990) as "storm-scoured pockets" colonised by brachiopods. Gutteridge (1990) based this interpretation on the sharp edges of the pockets truncating structures in the mud mound complex core, concentration of pockets towards the top of the mud mound complex core, and marked asymmetry of their bases. However, no evidence of storm scouring associated with the brachiopod-rich lenses was detected both at the outcrop and thin section scale. Lenses of brachiopod concentrations recognised in this study only rarely show sharp bases, do not display the pocket morphology described by Gutteridge (1990) and are homogeneously distributed in the mud mound complex core.

A revised interpretation based on the data provided in this study is that the brachiopod-rich lenses represent in fact centimetre- to decimetre-size depressions developed in the irregular mud mound complex core surface and colonised by brachiopods and fenestellid bryozoans. Precipitation of marine fibrous calcite cement resulted in the deposition of the skeletal grainstone/rudstone lithofacies (L8) characterising the lenses. The presence of subrounded automicrite intraclasts and the transitional boundary with the surrounding automicrite lithofacies (L7) suggests that L8 is contemporaneous with the mud mound complex core formation. Also, brachiopod assemblages in the lenses, which represent in situ life assemblages (sensu Brenchley and Harper 1998; Carniti et al. 2022) are the same as those occurring in association with the automicrite (L7, L9). This interpretation might apply also to other macrofaunal "pockets" in Mississippian mud mounds, e.g. the Tournaisian Waulsortian mud

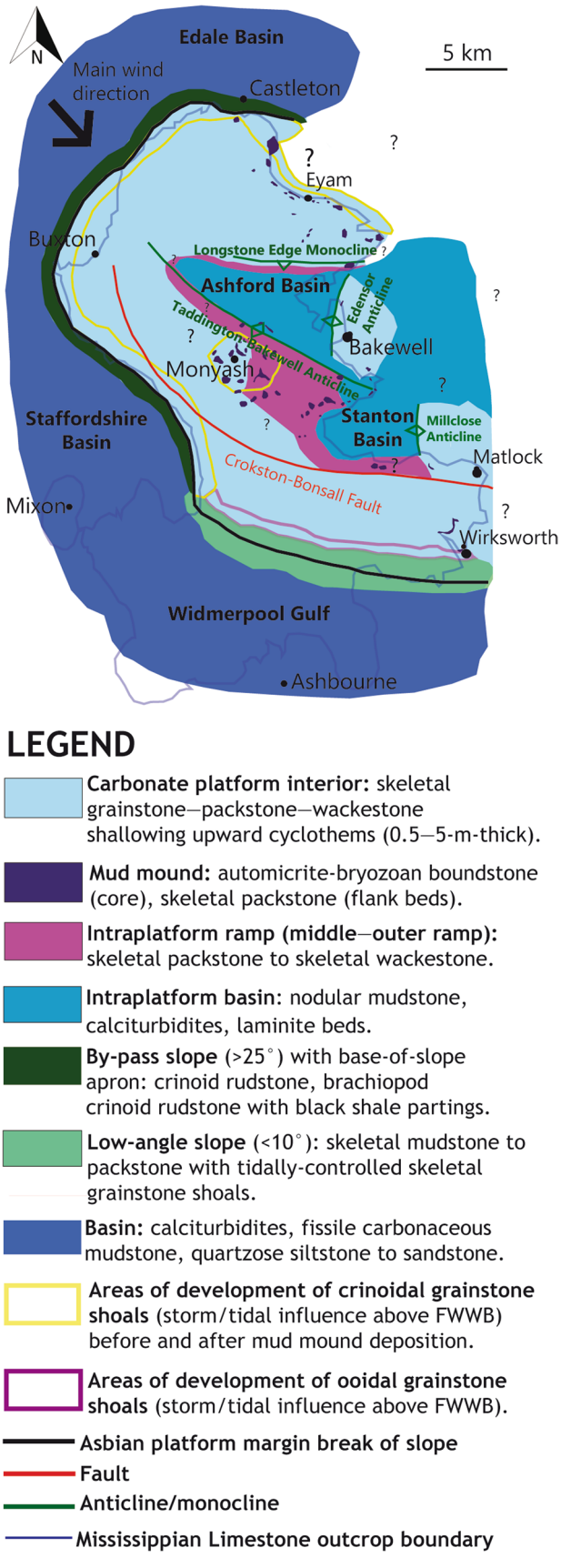

Fig. 14 Palinpastic reconstruction of the Peak District during growth of the mud mounds at the top of the Monsal Dale Limestone Formation in the latest Brigantian (late Visean). Reconstruction based upon regional data provided by Smith et al. (1967), Stevenson and Gaunt (1971), and Aitkenhead et al. (1985), integrated with data on the northern platform margin by Gawthorpe and Gutteridge (1990) and Harwood (2005), on the southern margin by Harwood (2005), on the Ashford Basin by Gutteridge (1987, 1989a), and on the area around Monyash by Gutteridge (1990, 1991, 1995) and Nolan et al. (2017). Data about the Asbian (upper Visean) margin of the Derbyshire Carbonate Platform from Harwood (2005) and Manifold et al. (2021). In the Monyash area, crinoidal grainstone shoals developed in inner-ramp settings overlie the mud mounds in the uppermost Monsal Dale Limestone Fm (Nolan et al. 2017) and in the Eyam Limestone Fm (Gutteridge 1989b; Nolan et al. 2017); they never occur underneath the mud mounds. The white box indicates the study area of Ricklow Quarry. *FWWB* Fair-weather wave base

mounds in the UK (Lees 1964) and USA (De Keyser 1978), and the upper Visean (Asbian) bioherms on the Derbyshire Carbonate Platform margin (Parkinson 1952).

The substrate variety in the mud mound complex sustained the high brachiopod diversity of the fauna (45 species, 36 genera, 7 orders; Table 3; Carniti et al. 2022). The mud mound complex surface likely was the site for both hard (bryozoan fronds, siliceous sponges, brachiopod shells) and soft (allomicrite) substrates, allowing colonisation of both pedicle-attached rhynchonellides, spiriferides, and terebratulides and seminfaunal concavo-convex productides. The surface depressions were likely the site of allomicrite concentration at their bases. This resulted in patchy soft substrates suitable for the colonisation by seminfaunal concavo-convex productides, whose shells were later colonised by pedicle-attached rhynchonellides, spiriferides, and terebratulides (taphonomic feedback).

Even though the role of brachiopods was limited to that of dwellers (sensu Fagerstrom 1988) in the mud mound complex, at Ricklow they were not limited to "pocket-like" concentrations, but were widespread. Brachiopods were a dominant skeletal component alongside fenestellid bryozoans and siliceous sponges, with which they were likely competing for space and resources (Carniti et al. 2022). The environment of the Ricklow mud mound complex had dispersed food resources (Carniti et al. 2022): the presence of abundant decaying organisms (siliceous sponges) and microbial mats likely resulted in more organic material in suspension on the mud mound surface with respect to off-mud mound complex, brachiopod-poor areas. This, in addition to scarcity of crinoids (which can access resources higher than brachiopods in the water column) and diverse hard and soft substrates enhanced brachiopod colonisation of the mud mound complex. Brachiopod shell abundance in turn provided hard substrates sustaining pedicle-attached brachiopods, bryozoans, sponges, and microbial mats (taphonomic feedback), contributing to and influencing mud mound growth and stability.

Comparison with other brachiopod-rich buildups

The mud mound complex at Ricklow Quarry differs from the Tournaisian Waulsortian mud mounds of Western Europe and USA (e.g. Somerville et al. 1992; Lees and Miller 1995) as it lacks any structured distribution of different mud generations (polymuds) and has a less extensive cavity system. Also, the Ricklow mud mound complex is dominated by clotted peloidal micrite, forming roughly 40% of the core volume, while Waulsortian mud mounds seem to be commonly dominated by "non-grumous micrite" (leiolite and allomicrite; Lees and Miller 1985; Devuyst and Lees 2001). The Ricklow mud mound complex also differs in skeletal assemblage: brachiopods in Waulsortian mud mounds are diverse (e.g. de Koninck 1887; Fraipont 1908; Demanet 1923, 1958; Mottequin and Simon 2017; Mottequin 2021), but few in all phases (Lees et al. 1985; Lees and Miller 1985, 1995), apparently always being less important than fenestellid bryozoans and crinoids.

The Ricklow mud mound complex markedly differs from Visean mud mounds consisting of encrusting trepostome bryozoans, serpulid, problematic worm tubes, and abundant brachiopods into automicrite ("microthrombolite" Bridges et al. 1995) classified as Type 5 buildups by Bridges et al. (1995) in having a much more diversified brachiopod fauna and no syndepositional mineralisation in the core. These mud mounds occur in eastern Canada (e.g. Dix and James 1987, 1989; Boehner 1989) and were developed in hydrothermal-seep vents related settings (von Bitter et al. 1990, 1992) at depths ranging from greater than 100 m to high-energy shallow waters (Webb 2002).

The Ricklow mud mound complex also differs from brachiopod-rich buildups with a framework built by calcimicrobes and fenestellid bryozoans occurring in the Lives Formation of north-eastern Belgium (Lauwers 1992; Chevalier and Aretz 2005), which developed in an inner-ramp setting, in lacking any calcimicrobe framework and having a more diverse skeletal composition and brachiopod fauna.

The Ricklow mud mound complex is similar to metre-scale brachiopod–bryozoan–ostracod mud mounds with micropeloidal mud textures developed on a carbonate ramp to the south of the Askrigg Block, northern Yorkshire, in the Holkerian–lower Asbian (middle–upper Visean), and in the flank facies of the Cracoean reefs developed on the same site in the upper Asbian (upper Visean) on the margin of a flat-topped carbonate platform (Mundy 2000; Waters et al. 2017). Also, the Ricklow mud mound complex is similar to the "bank facies" dominating the core of Cracoean reefs in Yorkshire (Mundy 1994) and Derbyshire (Harwood 2005), which consists of wackestone/floatstone with clotted micritic matrix hosting abundant brachiopods and corals alongside oncoids and dasycladacean algae. The Cracoean reefs show minor development in some areas (Waters et al. 2017) of a "framework facies" consisting of encrusting calcimicrobes, encrusting bryozoans, lithistid sponges, corals, shell-attached brachiopods, bivalves, and crinoids (Mundy 1994). Other buildups similar to Cracoean reefs occur along carbonate platform margins in the upper Visean of north-western Ireland (Somerville et al. 2009), Belgium (Muchez and Peeters 1987; Mottequin and Poty 2022), Turkey (Denayer and Aretz 2012), eastern Australia (Webb 1999), and in the upper Serpukhovian of Arkansas (Webb 1987), all of which host abundant and diverse brachiopod faunas.

Conversely, the Ricklow mud mound complex markedly differs from calcimicrobe–coral–lithistid sponge reefs in the Mississippian of Queensland, Australia (Shen and Webb 2005, 2008), microbial–bryozoan–coral reefs in the

upper Visean of Wales (Aretz and Herbig 2003), and microbial–sponge–bryozoan–coral reefs in the upper Visean of north-eastern Morocco (Aretz and Herbig 2008) in lacking any framework built by calcimicrobes, thrombolite/stromatolite (sensu Riding 2000) and/or corals, in having developed in deeper dysphotic settings and in having an abundant fauna of brachiopods.

Upper Visean Derbyshire mud mounds including the complex at Ricklow Quarry were considered as Type 3 crinoid–brachiopod–fenestellid bryozoan buildups by Bridges et al. (1995). Data provided in this study show that crinoids are not common in the mud mound complex core at Ricklow, while brachiopods and siliceous sponges are abundant and widespread in every lithofacies in the complex. A distinct sub-type of Type 3 buildups should here be defined to include the Ricklow mud mound complex, and likely other upper Visean Derbyshire mud mounds, characterised by abundant fenestellid bryozoans, brachiopods, and siliceous sponge spicules, few crinoids in the core, abundant clotted peloidal mud textures and no calcimicrobes. Other mud mounds referable to this newly defined sub-type developed around or below fair-weather wave base in the upper Visean (Brigantian) of the Midland Valley of Scotland (Shiells and Penn 1971; Brown 1977; Jameson 1980, 1987), and the upper Visean–Serpukhovian of the southern Montagne Noire, France (Poty et al. 2002; Vachard et al. 2017; Cózar et al. 2019a). Also referable to this sub-type they could be the brachiopod–bryozoan–ostracod mud mounds in the middle–upper Visean of Yorkshire (Waters et al. 2017). Conversely, other mud mounds considered as Type 3 buildups by Bridges et al. (1995) from the Visean of Ireland (Kelly and Somerville 1992), Scotland (Pickard 1992), and USA (Brown and Dodd 1990) differ from the Ricklow mud mound complex newly defined sub-type in having a different skeletal assemblage with few brachiopods, and usually abundant crinoids in the core.

In conclusion, brachiopods are a common skeletal constituent of Mississippian reefs, becoming increasingly important in middle–upper Visean buildups developed below fair-weather wave base in carbonate platform settings. Widespread development of buildups in platform settings in the middle–late Visean (Bridges et al. 1995) coincided, at least in Western Europe and North America (southern margin of Laurussia), with the evolution of Tournaisian ramps into flat-topped carbonate platforms (Gawthorpe 1986; Gawthorpe et al. 1989). Brachiopods are a dominant constituent of at least three types of Visean buildups in shallow platform settings: (1) calcimicrobe–bryozoan reefs (Chevalier and Aretz 2005), (2) Cracoean reefs (e.g. Mundy 1994), (3) fenestellid bryozoan–brachiopod–siliceous sponge mud mounds with common clotted peloidal micrite, a newly defined sub-type of Type 3 of Bridges et al. (1995), of which the Ricklow mud mound complex is a representative.

Water depth control on the abundance of brachiopods in Mississippian buildups is supported by the scarcity of brachiopods in middle–upper Visean mud mounds developed in middle–outer-ramp and basin settings such as in north-western Ireland (Kelly and Somerville 1992), the Béchar Basin in Algeria (Madi et al. 1996), and the eastern anti-Atlas in Morocco (Wendt et al. 2001). Also, the study by Cózar et al. (2019a) on the ecological distribution of skeletal grains in Serpukhovian buildups from the southern Montagne Noire in France, showed that brachiopod abundance increases with shallowing settings.

Substrate also played a role in controlling brachiopod colonisation of Mississippian carbonate buildups, as these were providing depressions in their irregular surface, muddy facies as well as firm, early cemented substrates more suitable for successful colonisation by brachiopods with respect to packstone to grainstone mobile substrates in the surrounding platform interior settings (cf. Webb 2001, for coral mud mound colonisation).

Occurrence of microbial mats and decaying siliceous sponge tissues in the buildups (cf. Brunton and Dixon 1994) likely provided also more abundant food resources than in the surrounding areas. In upper Visean Cracoean reefs and fenestellid bryozoan–brachiopod–siliceous sponge mud mounds productide brachiopods seem to dominate the fauna (Webb 1987; Brunton and Mundy 1988; Brunton and Tilsley 1991; Mottequin and Poty 2022; Carniti et al. 2022). This might be indicative of dispersed food resources (Pérez-Huerta and Sheldon 2006), a condition that markedly differs from the eutrophic settings related to upwelling currents where Waulsortian mud mounds developed in the late Tournaisian (Lees and Miller 1985, 1995).

Hence, it was probably a combination of relative shallow depths between fair-weather and storm wave base, moderate-energy, diverse substrate types, and distribution of food resources that favoured the brachiopod colonisation and in turn the structuring of brachiopod-rich buildups in the middle–upper Visean.

Conclusions

Lithofacies and brachiopod faunal distribution analysis of the upper Visean (Brigantian) mud mound complex of Ricklow Quarry, developed on the Derbyshire Carbonate Platform at the top of the Monsal Dale Limestone Fm led to a reinterpretation of its lithofacies architecture and depositional model. The Ricklow mud mound complex originated during a period of creation of accommodation in an intra-platform middle-ramp dysphotic environment with dispersed

food resources. The mud mound complex growth was interrupted by a subaerial exposure due to a relative sea-level fall.

Brachiopods are not, as previously reported, limited to storm-scoured isolated pockets (Gutteridge 1990, 1995), and are widespread in every lithofacies of the mud mound complex of Ricklow. Brachiopod abundance provided hard substrates for other sessile organisms and contributed to mud mound growth. Brachiopod-richer lenses do exist in the mud mound complex core and are reinterpreted as the result of brachiopod colonisation of depressions in the irregular sea floor surface of the mud mound complex core.

The Ricklow mud mound complex represents a newly defined middle–upper Visean sub-type of Bridges et al. (1995) Type 3 buildups: fenestellid bryozoan–brachiopod–siliceous sponge mud mounds. These mud mounds developed in Western European platform settings below fair-weather wave base, in environments with dispersed food resources.

This study demonstrates the important role of brachiopods in Mississippian buildups, and the importance of characterising their distribution and diversity to enhance understanding of Mississippian reef diversity, evolution, and depositional environments.

Acknowledgements The authors are grateful to Martina Bruno, who contributed to the fieldwork through her master thesis project, Curzio Malinverno and Matteo Pegoraro (University of Milan) for preparing thin sections for petrographic analysis, the British Geological Survey staff for hosting APC in their facilities and for sample shipping to Italy, and Natural England for study permits for the Ricklow Quarry site, part of the Lathkill Dale SSSI. Markus Aretz and an anonymous reviewer are thanked for their valuable comments, which have led to improvements in the manuscript.

Funding Open access funding provided by Università degli Studi di Milano within the CRUI-CARE Agreement. Financial support was provided by PhD grant from University of Milan and MUR Italian Ministry of University.

Data availability The materials used for this study are housed in the collection of the Museum of Palaeontology of the Department of Earth Sciences "A. Desio", Università degli Studi di Milano, Milan, Italy, and are labelled MPUM12295.

Declarations

Conflict of interest There are no conflicts of interest and data are available on request to the corresponding author.

References

Adams AE (1980) Calcrete profiles in the Eyam Limestone (Carboniferous) of Derbyshire: petrology and regional significance. Sedimentology 27:651–660. https://doi.org/10.1111/j.1365-3091.1980.tb01653.x

Adams AE (1984) Development of algal-foraminiferal-coral reefs in the Lower Carboniferous of Furness, north west England. Lethaia 17:233–249. https://doi.org/10.1111/j.1502-3931.1984.tb01623.x

Aitkenhead N, Chisholm JI (1982) A standard nomenclature for the Dinantian formations of the Peak District of Derbyshire and Staffordshire. Inst Geol Sc, London, p 18

Aitkenhead N, Chisholm JI, Stevenson IP, Mitchell M, Strank ARE, Cornwell JD, Berridge NG (1985) Geology of the country around Buxton, Leek and Bakewell: Memoir for 1:50.000 geological Sheet 111 (England and Wales). HMSO, London, p. 168

Aitkenhead N, Barclay WJ, Brandon A, Chadwick RA, Chisholm JI, Cooper AH, Johnson EW (2002) British regional geology: the Pennines and adjacent areas (Fourth edition). HMSO, London, p 206

Angiolini L (2007) Quantitative palaeoecology in the *Pachycyrtella* Bed, Early Permian of Interior Oman. Palaeoworld 16:233–245. https://doi.org/10.1016/j.palwor.2007.05.019

Angiolini L, Crippa G, Azmy K, Capitani G, Confalonieri G, Della Porta G, Griesshaber E, Harper DAT, Leng MJ, Nolan L, Orlandi M, Posenato R, Schmahl WW, Banks VJ, Stephenson MH (2019) The giants of the phylum brachiopoda: a matter of diet? Palaeontology 62:889–917. https://doi.org/10.1111/pala.12433

Angiolini L, Cisterna GA, Mottequin B, Shen SZ, Muttoni G (2021) Global Carboniferous brachiopod biostratigraphy. In: Lucas SG, Schneider JW, Wang X, Nikolaeva S (eds) The Carboniferous Timescale. Geol Soc Sp Publ No 512, pp 497–550. https://doi.org/10.1144/SP512-2020-225

Aretz M, Chevalier E (2007) After the collapse of stromatoporid–coral reefs—the Famennian and Dinantian reefs of Belgium: much more than Waulsortian mounds. In: Alvaro JJ, Aretz M, Boulvain F, Munnecke A, Vachard D, Vennin E (eds) Palaeozoic reefs and bioaccumulations: climatic and evolutionary controls. Geol Soc Spec Publ No 275, pp 163–188. https://doi.org/10.1144/GSL.SP.2007.275.01.1

Aretz M, Herbig HG (2003) Coral-Rich Bioconstructions in the Viséan (Late Mississippian) of Southern Wales (Gower Peninsula, UK). Facies 49:221–242. https://doi.org/10.1007/s10347-003-0033-y

Aretz M, Herbig HG (2008) Microbial-sponge and microbial-metazoan buildups in the Late Viséan basin-fill sequence of the Jerada Massif (Carbonifeorus, NE Morocco). Geol J 43:307–336. https://doi.org/10.1002/gj.1120

Aretz M, Webb GE (2007) Western European and eastern Australian Mississippian shallow-water reefs: a comparison. In: Wong ThE (ed.) Proceedings of the XVth International Congress on Carboniferous and Permian Stratigraphy, Utrecht 2003, pp 433–442

Aretz M, Poty E, Devuyst FX, Hance L, Hou H (2012) Late Tournaisian Waulsortian-like carbonate mud banks from South China (Longdianshan Hill, central Guangxi): preliminary investigations. Geol Jour 47:450–461. https://doi.org/10.1002/gj.2459

Aretz M, Legrand-Blain M, Vachard D, Izart A (2019) Gigantoproductid and allied productid brachiopods from the 'Calcaires à *Productus*' (late Viséan—Serpukhovian; Montagne Noire, southern France): taxonomy and palaeobiogeographical position in

the Palaeotethys. Geobios 55:17–40. https://doi.org/10.1016/j.geobios.2019.06.007
Aretz M, Herbig HG, Wang X, Gradstein FM, Agterberg FG, Ogg JG (2020) The Carboniferous period. In: Gradstein FM, Ogg JG, Schmitz MD, Ogg GM (eds) The Geologic Time Scale 2020. Elsevier, Amsterdam, pp 811–874
Ausich WI, Meyer DL (1990) Origin and composition of carbonate buildups and associated facies in the Fort Payne Formation (Lower Mississippian, south-central Kentucky): An integrated sedimentologic and palaeoecologic analysis. Bull Geol Soc Am 102:129–146. https://doi.org/10.1130/0016-7606(1990)102%3c0129:OACOCB%3e2.3.CO;2
Baccelle L, Bosellini A (1965) Diagrammi per la stima visiva della composizione percentuale delle rocce sedimentarie. Ann Uni Ferrara NS Sez IX Sci Geol Paleont 1:59–62
Bancroft AJ, Somerville ID, Strank AE (1988) A bryozoan buildup from the Lower Carboniferous of North Wales. Lethaia 21:51–65. https://doi.org/10.1111/j.1502-3931.1988.tb01753.x
Biggins D (1969) The structure, sedimentology and palaeoecology of a Carboniferous knoll at High Tor, Derbyshire. PhD thesis, Chelsea College, University of London, London, p. iv+261
Boehner RC (1989) Carbonate buildups of the Windsor Group Major Cycle: Maxner and Miller Limestones, Miller Creek Formation and Mosher Road Member, Elderbank Formation and B2 Limestone, Nova Scotia. In: Geldsetzer HHJ, James NP, Tebbutt GE (eds) Reefs, Canada & Adjacent Area. Mem Can Soc Petrol Geol No 13, pp 600–608
Boehner RC, Giles PS, Wray DAM, Ryan RJ (1989) Carbonate buildups of the Gays River Formation, Lower Carboniferous Windsor Group, Nova Scotia. In: Geldsetzer HHJ, James NP, Tebbutt GE (eds) Reefs, Canada & Adjacent Area. Mem Can Soc Petrol Geol No 13, pp 609–621
Bosence DWJ, Bridges PH (1995) A review of the origin and evolution of carbonate mud-mounds. In: Monty CL, Bosence DWJ, Bridges PH, Pratt BR (eds) Carbonate mud mounds: their origin and evolution. Int Ass Sed Sp Publ No 23, pp 3–10
Bourque PA, Boulvain F (1993) A model for the origin and petrogenesis of the red stromatactis limestone of Paleozoic carbonate mounds. J Sed Petrol 63:607–619. https://doi.org/10.1306/D4267B8B-2B26-11D7-8648000102C1865D
Braga JC, Martin JM, Riding R (1995) Controls on microbial dome fabric development along a carbonate-siliciclastic shelf-basin transect, Miocene, SE Spain. Palaios 10:347–361. https://doi.org/10.2307/3515160
Brenchley PJ, Harper D (1998) Palaeoecology: ecosystems, environments and evolution. Chapman and Hall, London, p 400
Bridges PH (1982) The origin of cyclothems in the late Dinantian platform carbonates at Crich, Derbyshire. Proc York Geol Soc 44:159–180. https://doi.org/10.1144/pygs.44.2.159
Bridges PH, Chapman AJ (1988) The anatomy of a deep water mud mound complex to the southwest of the Dinantian platform in Derbyshire, UK. Sedimentology 35:141–162. https://doi.org/10.1111/j.1365-3091.1988.tb00909.x
Bridges PH, Gutteridge P, Pickard NAH (1995) The environmental setting of Early Carboniferous mud mounds. In: Monty CLV, Bosence DWJ, Bridges PH, Pratt BR (eds) Carbonate mud mounds: their origin and evolution. IAS Sp Publ No 23, pp 171–190. https://doi.org/10.1002/9781444304114.ch6
Broadhurst FM, Simpson IM (1973) Bathymetry on a Carboniferous reef. Lethaia 6:367–381. https://doi.org/10.1111/j.1502-3931.1973.tb01204.x
Brown SS (1977) The petrogenesis and depositional environment of the Dockra Limestone (Upper Visean), North Ayrshire. PhD thesis, University of Glasgow, Glasgow, p. 150
Brown MA, Dodd JR (1990) Carbonate mud bodies in middle Mississippian strata of southern Indiana and northern Kentucky: end members of a middle Mississippian mud mound spectrum? Palaios 5:236–243. https://doi.org/10.2307/3514942
Brunton CHC (1982) British Dinantian (Lower Carboniferous) *Terebratulid brachiopods*. Bull Brit Mus (Nat Hist) Geol 36:45−57
Brunton FR, Dixon O (1994) Siliceous sponge–microbe biotic associations and their recurrence through the Phanerozoic as reef mound constructors. Palaios 4:370–387. https://doi.org/10.2307/3515056
Brunton CHC, Lazarev SS (1997) Evolution and classification of the Productellidae (Productida), upper Paleozoic brachiopods. J Pal 7:381−394
Brunton CHC, Mundy DJC (1988) Strophalosiacean and aulostegacean productoids (Brachiopoda) from the Craven Reef Belt (late Viséan) of North Yorkshire. Proc York Geol Soc 47:55–88. https://doi.org/10.1144/pygs.47.1.55
Brunton CHC, Tilsley JW (1991) A check list of brachiopods from Treak Cliff, Derbyshire, with reference to other Dinantian (Lower Carboniferous) localities. Proc York Geol Soc 48:287–295. https://doi.org/10.1144/pygs.48.3.287
Buggisch W (1991) The global Frasnian–Famennian 'Kellwasser event.' Geol Rundsch 80:49–72. https://doi.org/10.1007/BF01828767
Burchette TP, Wright VP (1992) Carbonate ramp depositional systems. Sediment Geol 79:3–57. https://doi.org/10.1016/0037-0738(92)90003-A
Butcher NJD, Ford TD (1973) The Carboniferous Limestone of Monsal Dale, Derbyshire. Merc Geol 4:179–195
Carniti AP, Della Porta G, Banks VJ, Stephenson MH, Angiolini L (2022) Brachiopod fauna from upper Visean, Mississippian, mud mounds in Derbyshire, UK. Acta Pal Pol 67:865–915. https://doi.org/10.4202/app.00972.2022
Chevalier E, Aretz M (2005) A microbe bryozoan reef from the middle Viséan of the Namur Syncline (Engihoul Quarry). Geol Belg 8:109–119
Conil R (1980) Note sur quelques foraminifères du Strunien et du Dinantien d'Europe occidentale. Ann Soc Géol Belg 103:43–53
Cotter E (1965) Waulsortian-type carbonate banks in the Mississippian Lodgepole Formation of central Montana. J Geol 73:881–888. https://doi.org/10.1086/627125
Cox FC, Bridge DMC, Chisholm JI, Aitkenhead N (1977) The limestone and dolomite resources of the country around Monyash, Derbyshire. Description of 1:25,000 resource sheet SK 16. Institute of Geological Sciences, London, p 137
Cózar P, Somerville ID (2014) Latest Viséan—Early Namurian (Carboniferous) foraminifers from Britain: implications for biostratigraphic and glacioeustatic correlations. News Strat 47(3):355–367. https://doi.org/10.1127/nos/2014/0052
Cózar P, Somerville ID (2021) Foraminifers in upper Viséan-lower Serpukhovian limestones from South Wales: regional correlation and implications for the British foraminiferal zonal schemes. Proc York Geol Soc 63: https://doi.org/10.1144/pygs2020-009
Cózar P, Vachard D, Aretz M, Somerville ID (2019a) Foraminifers of the Viséan-Serpukhovian boundary interval in Western Palaeotethys: a review. Lethaia 52:260–284. https://doi.org/10.1111/let.12311
Cózar P, Izart A, Somerville ID, Aretz M, Coronado I, Vachard D (2019b) Environmental controls on the development of Mississippian microbial carbonate mounds and platform limestones in southern Montagne Noire (France). Sedimentology 66:2392–2424. https://doi.org/10.1111/sed.12594
Davidson T (1858−1863) Monograph of British Fossil Brachiopoda. Vol. II, Part. V: The Carboniferous Brachiopoda. Mon Palaeont Soc 10−14 (42, 46, 54, 55, 59):81−280
de Koninck LG (1842−1844) Description des animaux fossils qui se trouvent dans le terrain Carbonifère de Belgique. H. Dessain, Liege, p 650

de Koninck LG (1887) Faune du calcaire carbonifère de la Belgique. Sixième partie. Brachiopodes. Ann Musée Royal Hist Nat Belg 14:1–154

Della Porta G, Kenter JA, Immenhauser A, Bahamonde JR (2002) Lithofacies character and architecture across a Pennsylvanian inner-platform transect (Sierra de Cuera, Asturias, Spain). J Sed Res 72:898–916. https://doi.org/10.1306/040902720898

Della Porta G, Villa E, Kenter JAM (2005) Facies distribution of fusulinida in a Bashkirian-Moscovian (Pennsylvanian) carbonate platform top (Cantabrian Mountains, NW Spain). J Foram Res 35:344–367. https://doi.org/10.2113/35.4.344

Demanet F (1923) Le Waulsortien de Sosoye et ses rapports fauniques avec le Waulsortien d'âge Tournaisien supérieur. Mém Inst Géol Université De Louvain 2:37–285

Demanet F (1958) Contribution à l'étude du Dinantien de la Belgique. Mém Inst Royal Sc Nat Bel 141:1–152

Denayer J, Aretz M (2012) Discovery of a Mississippian reef in Turkey: The Upper Viséan Microbial-Sponge-Bryozoan-Coral Bioherm From Kongul Yayla (Taurides, S Turkey). Turk J Earth Sc 21:375–389. https://doi.org/10.3906/yer-1008-3

Devuyst FX, Lees A (2001) The initiation of Waulsortian buildups in Western Ireland. Sedimentology 48:1121–1148

Dix GR, James NP (1987) Late Mississippian bryozoan/microbial build-ups on a drowned karst terrain: Port au Port Peninsula, western Newfoundland. Sedimentology 34:779–793. https://doi.org/10.1111/j.1365-3091.1987.tb00802.x

Dix GR, James NP (1989) Upper Mississippian bryozoan/microbial bioherms, western Newfoundland. In: Geldsetzer HHJ, James NP, Tebbutt GE (eds) Reefs, Canada and adjacent area. Canad Soc Petrol Geol Mem No 13, pp 667–671

Dunham RJ (1962) Classification of carbonate rocks according to depositional texture. In: Ham WE (ed) Classification of carbonate rocks, a symposium No 1, pp 108–171

Dupont E (1881) Sur l'origine des calcaires dévoniens de la Belgique. Bull Acad Roy Sci Belg Third Ser 2:264–280

Dupraz C, Visscher PT, Baumgartner LK, Reid RP (2004) Microbe-mineral interactions: early carbonate precipitation in a hypersaline lake (Eleuthera Island, Bahamas). Sedimentology 51:745–765. https://doi.org/10.1111/j.1365-3091.2004.00649.x

Dupraz C, Reid RP, Braissant O, Decho AW, Norman RS, Visscher PT (2009) Processes of carbonate precipitation in modern microbial mats. Earth Sc Rev 96:141–162. https://doi.org/10.1016/j.earscirev.2008.10.005

Embry AF, Klovan JE (1971) A late Devonian reef tract on northeastern banks island, nwt. Bull Canad Petrol Geol 19:730–781. https://doi.org/10.35767/gscpgbull.19.4.730

Fagerstrom JA (1988) A structural model for reef communities. Palaios 3:217–220. https://doi.org/10.2307/3514531

Fielding C, Frank T, Birgenheier L, Rygel MC, Jones AT, Roberts J (2008) Stratigraphic imprint of the Late Palaeozoic Ice Age in eastern Australia: a record of alternating glacial and nonglacial climate regime. J Geol Soc 165:129–140. https://doi.org/10.1144/0016-76492007-036

Fleming J (1828) A history of British animals. Bell and Bredfute, Edinburgh, p 265. https://doi.org/10.5962/bhl.title.12859

Flügel E (2004) Microfacies of carbonate rocks. Springer, Berlin. https://doi.org/10.1007/978-3-642-03796-2

Flügel E, Kiessling W (2002) A new look at ancient reefs. In: Kiessling W, Flügel E, Golonka J (eds) Phanerozoic reef patterns. SEPM Special Publications No 72, pp 3–10.

Fraipont C (1908) Notes sur quelques fossiles du Calcaire carbonifère. Ann Soc Géol Bel (mém) 35:7–12

Frankel RB, Bazylinski DA (2003) Biologically induced mineralization by bacteria. In: Dove PM, Weiner S, De Yoreo JJ (eds) Biomineralization. Mineralogical Society of America, Review in Mineralogy and Geochemistry 54, pp 95–114. Washington, D.C.

Fritz GK (1958) Schwammstotzen, Tuberolithe und Schuttbreccien im weiißen Jura der schwäbischen Alb. Arb Geol Paläont Instt Tech Hochschule Stuttgart 13:113

Gallagher SJ (1988) Controls on the distribution of calcareous Foraminifera in the Lower Carboniferous of Ireland. Mar Micropal 34:187–211. https://doi.org/10.1016/S0377-8398(98)00006-1

Gallagher SJ, Somerville ID (2003) Lower Carboniferous (late Visean) platform development and cyclicity in southern Ireland: foraminiferal biofacies and lithofacies evidence. Riv Ita Pal Strat 109:159–171. https://doi.org/10.13130/2039-4942/5499

Gawthorpe RL (1986) Sedimentation during carbonate ramp to slope evolution in a tectonically active area: Bowland Basin (Dinantian), northern England. Sedimentology 33:185–205. https://doi.org/10.1111/j.1365-3091.1986.tb00531.x

Gawthorpe RL, Gutteridge P (1990) Geometry and evolution of platform margin bioclastic shoals, late Dinantian (Mississippian), Derbyshire, UK. In: Tucker ME, Wilson PD, Crevello JR, Sarg JR, Read JF (eds) Carbonate platforms: facies, sequences and evolution. IAS Sp Publ No 9, pp 39–54. https://doi.org/10.1002/9781444303834.ch2

Gawthorpe RL, Gutteridge P, Leeder MR (1989) Late Devonian and Dinantian basin evolution in northern England and North Wales. In: Arthurton RS, Gutteridge P, Nolan SC (eds) The role of tectonics and Carboniferous sedimentation in the British Isles. Proc York Geol Soc Occ Publ No 6, pp 1–23

George TNG (1932) The British Carboniferous reticulate spiriferidae. Quart J Geol Soc 88:516−574. https://doi.org/10.1144/GSL.JGS.1932.088.01-04.1

Guido A, Heindel K, Birgel D, Rosso A, Mastandrea A, Sanfilippo R, Russo F, Peckmann J (2013) Pendant bioconstructions cemented by microbial carbonate in submerged marine caves (Holocene, SE Sicily). Palaeogeogr Palaeoclimatol Palaeoecol 388:166–180. https://doi.org/10.1016/j.palaeo.2013.08.007

Guido A, Rosso A, Sanfilippo R, Miriello D, Belmonte G (2022) Skeletal vs microbialite geobiological role in bioconstructions of confined marine environments. Palaeogeogr Palaeoclimatol Palaeoecol 593:110920. https://doi.org/10.1016/j.palaeo.2022.110920

Guion PD, Fielding C (1988) Westphalian A and B sedimentation. In: Besly BM, Kelling G (eds) Sedimentation in a synorogenic basin complex; the Upper Carboniferous of NW Europe. Blackie, Glasgow, pp 153–177

Guion PD, Gutteridge P, Davies SJ (2000) Carboniferous sedimentation and volcanism on the Laurussian margin. In: Woodcock N, Strachan R (eds) Geological history of Britain and Ireland. Blackwell Science, Oxford, pp 227–270

Gutteridge P (1987) Dinantian sedimentation and the basement structure of the Derbyshire Dome. Geol J 22:25–41. https://doi.org/10.1002/gj.3350220104

Gutteridge P (1989a) Controls on carbonate sedimentation in a Brigantian intrashelf basin (Derbyshire). In: Arthurton RS, Gutteridge P, Nolan SC (eds) The role of tectonics and Carboniferous sedimentation in the British Isles. Proc York Geol Soc Occ Publ No 6, pp 171–187

Gutteridge P (1989b) Shark predation of Dinantian brachiopods from the Derbyshire Dome. Mercian Geol 11:237–244

Gutteridge P (1990) The origin and significance of shelly macrofauna in late Dinantian carbonate mud mounds of Derbyshire. Proc York Geol Soc 48:23–32. https://doi.org/10.1144/pygs.48.1.23

Gutteridge P (1991) Revision of the Monsal Dale/Eyam Limestone boundary (Dinantian) in Derbyshire. Merc Geol 12:71–78

Gutteridge P (1995) Late Dinantian (Brigantian) Carbonate Mud Mounds of the Derbyshire Carbonate Platform. In: Monty CLV, Bosence DWJ, Bridges PH, Pratt BR (eds) Carbonate mud mounds: their origin and evolution. IAS Sp Publ No 23, pp 298–307. https://doi.org/10.1002/9781444304114.ch9

Gutteridge P (2003) A record of the Brigantian limestone succession in the partly infilled Dale Quarry, Wirksworth. Merc Geol 15:219–224

Harper DAT, Jeffrey AL (1996) Mid-Dinantian brachiopod biofacies from western Ireland. In: Somerville P, Jones GL (eds) Recent Advances in Lower Carboniferous Geology. Geol Soc Spec Publ No 107, pp 427–436. https://doi.org/10.1144/GSL.SP.1996.107.01.30

Harwood M (2005) Facies architecture and depositional geometry of a late Viséan carbonate platform margin, Derbyshire, UK. PhD thesis, Cardiff University, p. 295

Herbig HG (2016) Mississippian (Early Carboniferous) sequence stratigraphy of the Rhenish Kulm Basin, Germany. Geol Bel 19:81–110. https://doi.org/10.20341/gb.2016.010

Horbury AD (1989) The relative roles of tectonism and eustasy in the deposition of the Urswick Limestone Formation in south Cumbria and north Lancashire. In: Arthurton RS, Gutteridge P, Nolan SC (eds) The Role of Tectonics in Devonian and Carboniferous Sedimentation in the British Isles. York Geol Soc Occ Publ No 6, pp 153–169

Horbury AD (1992) A late Dinantian peloid cementstone-palaeoberesellid buildup from north Lancashire, England. Sediment Geol 79:117–137. https://doi.org/10.1016/0037-0738(92)90007-E

Isbell JL, Miller MF, Wolfe KL, Lenaker PA (2003) Timing of late Paleozoic glaciation in Gondwana: Was glaciation responsible for the development of Northern Hemisphere cyclothems? In: Chan MA, Archer AW (eds) Extreme depositional environments: mega end members in geologic time. Geol Soc Am Spec Paper No 370, pp 5–24. https://doi.org/10.1130/0-8137-2370-1.5

James NP (1978) Facies models 10. Reefs Geoscience Canada No 5, pp 16–26

James NP (1983) Reef environment. In: Scholle PA, Bebout DG, Moore CH (eds) Am Assoc Pet Geol Mem No 33, pp 346–440

James NP, Bourque PA (1992) Reefs and mounds. In: Walker RG, James NP (eds) Facies models, response to sea level change. Geol Assoc Can, Geotext No 1, pp 323–347

Jameson J (1980) Depositional environments in the Petershill Formation, Bathgate, West Lothian. PhD thesis, University of Edinburgh, p 544

Jameson J (1987) Carbonate sedimentation on a mid-basin high: the Petershill Formation, Midland Valley of Scotland. In: Miller J, Adams AE, Wright VP (eds) European Dinantian Environments. Geol J Spec Issue No 12, pp 309–327

Kelly JG, Somerville ID (1992) Arundian (Dinantian) carbonate mudbanks in north-west Ireland. Geol J 27:221–241. https://doi.org/10.1002/gj.3350270303

Kendall AC (1985) Radiaxial fibrous calcite: a reappraisal. In: Schneidermann N, Harris PM (eds) Carbonate cements. SEPM Spec Publ No 36, pp 59–77

Keupp H, Jenisch A, Herrmann R, Neuweiler F, Reitner J (1993) Microbial carbonate crusts—a key to the environmental analysis of fossil spongiolites? Facies 29:41–54. https://doi.org/10.1007/BF02536916

De Keyser TL (1978) The Early Mississippian of the Sacramento Mountains, New Mexico – an Ecofacies Model for Carbonate Shelf Margin Deposition. PhD thesis, Oregon State University, p. 304

Lauwers AS (1992) Growth and diagenesis of cryptalgal-bryozoan buildups within a mid-Viséan (Dinantian) cyclic sequence, Belgium. Ann Soc Géol Belg 115:187–213

Lee JH, Riding R (2020) The 'classic stromatolite' Cryptozoön is a keratose sponge-microbial consortium. Geobiology 19:189–198. https://doi.org/10.1111/gbi.12422

Leeder MR (1976) Sedimentary Facies and the Origins of Basin Subsidence along the Northern Margin of the Supposed Hercynian Ocean. Dev Geotect 12:167–179. https://doi.org/10.1016/B978-0-444-41549-3.50016-5

Leeder MR (1982) Upper Palaeozoic basins of the British Isles—Caledonite inheritance versus Hercynian plate margin processes. J Geol Soc Lond 139:479–490. https://doi.org/10.1144/gsjgs.139.4.047

Lees A (1964) The structure and origin of the Waulsortian reefs of west-central Eire. Ph Trans R Soc London Ser. B 247:483–531. https://doi.org/10.1098/rstb.1964.0004

Lees A (1988) Waulsortian 'reefs': the history of a concept. Mem Inst Geol Univ Louvain 34:43–55

Lees A (1997) Biostratigraphy, sedimentology and palaeobathymetry of Waulsortian buildups and peri-Waulsortian rocks during the late Tournaisian regression, Dinant area, Belgium. Geol J 32:1–36. https://doi.org/10.1002/(SICI)1099-1034(199703)32:1%3c1::AID-GJ715%3e3.0.CO;2-0

Lees A, Miller J (1985) Facies variation in Waulsortian buildups, part. 2; mid-Dinantian buildups from Europe and North America. Geol J 20:159–180. https://doi.org/10.1002/gj.3350200207

Lees A, Miller J (1995) Waulsortian banks. In: Monty CLV, Bosence DWJ, Bridges PH, Pratt BR (eds) Carbonate mud mounds: their origin and evolution. IAS Sp Publ No 23, pp 191–271. https://doi.org/10.1002/9781444304114.ch7

Lees A, Hallet V, Hibo D (1985) Facies variation in Waulsortian buildups, part 1; a model from Belgium. Sedimentology 20:133–158. https://doi.org/10.1002/gj.3350200206

Lucas SG, Schneider JW, Nikolaeva S, Wang X (2022) The Carboniferous timescale: an introduction. In: Lucas SG, Schneider JW, Wang X, Nikolaeva S (eds) The Carboniferous Timescale. Geol Soc London Sp Publ No 512, pp 1–17. https://doi.org/10.1144/SP512-2021-160

Madi A, Bourque PA, Mamet B (1996) Depth-related ecological zonation of a Carboniferous Carbonate ramp: Upper Viséan of Béchar Basin, Western Algeria. Facies 35:59–80. https://doi.org/10.1007/BF02536957

Manifold L, Hollis C, Burgess P (2020) The Anatomy of a Mississippian (Viséan) carbonate platform interior, UK: depositional cycles, glacioeustasy and facies mosaics. Sediment Geol 401:105633. https://doi.org/10.1016/j.sedgeo.2020.105633

Manifold L, Del Strother P, Gold DP, Burgess P, Hollis C (2021) Unravelling Evidence for Global Climate Change in Mississippian Carbonate Strata from the Derbyshire and North Wales Platforms, UK. J Geol Soc 2:2. https://doi.org/10.1144/jgs2020-106

Martin W (1809) Petrificata derbiensa; Figures and descriptions of petrefactions collected in derbyshire. Wigan, London, p 28. https://doi.org/10.5962/bhl.title.119699

McConnaughey T (1989) Biomineralization mechanisms. In: Crick RE (ed.) Origin, evolution, and modern aspects of biomineralization in plants and animals. Plenum, New York, pp 57–73

McIntosh MJ (1974) Some Scottish Carboniferous davidsoniacean brachiopods. Scot Jour Geol 10:199−222. https://doi.org/10.1144/sjg10030199

Meyer DL, Ausich WI, Bohl DT, Norris WA, Potter PE (1995) Carbonate mud mounds in the Fort Payne Formation (lower Carboniferous) Cumberland Saddle region, Kentucky and Tennessee, USA. In: Monty CLV, Bosence DWJ, Bridges PH, Pratt BR (eds) Carbonate mud mounds: their origin and evolution. IAS Sp Publ No 23, pp 273–287. https://doi.org/10.1002/9781444304114.ch9

Miller J, Grayson RF (1972) Origin and structure of the Lower Viséan 'reef' limestones near Clitheroe, Lancashire. Proc York Geol Soc 38:607–638. https://doi.org/10.1144/pygs.38.4.607

Monty CLV (1995) The rise and nature of carbonate mud mounds: an introductory actualistic approach. In: Monty CLV, Bosence DWJ, Bridges PH, Pratt BR (eds) Carbonate mud mounds; their origin

and evolution. IAS Sp Publ No 23, pp 11–48. https://doi.org/10.1002/9781444304114.ch2
Mottequin B (2021) Earth science collections of the Centre Grégoire Fournier (Maredsous) with comments on Middle Devonian-Carboniferous brachiopods and trilobites from southern Belgium. Geol Bel 24:33–68. https://doi.org/10.20341/gb.2020.028
Mottequin B, Poty E (2022) Brachiopods from the historical type area of the Viséan Stage (Carboniferous, Mississippian; Belgium) and the Visé fauna: preliminary remarks. Palaeodiv Palaeoenv 102:351–371. https://doi.org/10.1007/s12549-021-00498-9
Mottequin B, Simon E (2017) New insights on Tournaisian-Visean (Carboniferous, Mississippian) athyridide, orthotetide, rhynchonellide, and strophomenide brachiopods from southern Belgium. Pal Elect 20:1–45
Muchez P, Peeters C (1987) The occurrence of a cryptalgal reef structure in the upper Viséan of the Visé area. Ann Soc Géol Belg 109:573–577
Muir-Wood HM (1928) British Carboniferous Producti, 2. *Productus* sensu stricto *Semireticulatus* and *Longispinus* group. Mem Geol Surv UK Palaeont 3:3–217
Mundy DJC (1994) Microbialite-sponge-bryozoan-coral framestones in the Lower Carboniferous (Upper Viséan) buildups of northern England (UK). In: Beauchamp B, Emery AF, Glass DJ (eds) Pangea: Global Environments and Resources, Can Soc Petrol Geol Mem No 17, pp 713–729
Mundy DJC (2000) Field meeting to the Craven Reef Belt: Settle and Cracoe Sunday, 23rd July 2000. Talisman Energy Inc., Calgary
Neuweiler F, Burdige DJ (2005) The modern calcifying sponge *Spheciospongia vesparium* (Lamarck, 1815), Great Bahama Bank: implications for ancient sponge mud-mounds. Sediment Geol 175:89–98. https://doi.org/10.1016/j.sedgeo.2004.12.021
Neuweiler F, Daoust I, Bourque PA, Burdige DJ (2007) Degradative calcification of a modern siliceous sponge from the Great Bahama bank, the Bahamas: a guide for interpretation of ancient sponge-bearing limestone. J Sed Res 77:552–563. https://doi.org/10.2110/jsr.2007.058
Nolan LSP, Angiolini L, Jadoul F, Della Porta G, Davies SJ, Banks VJ, Stephenson MH, Leng MJ (2017) Sedimentary context and palaeoecology of *Gigantoproductus* shell beds in the Mississippian Eyam Limestone Formation, Derbyshire carbonate platform, central England. Proc York Geol Soc 61:239–257. https://doi.org/10.1144/pygs2017-393
Orme GR (1971) The D_2-P_1 "reef" and associated limestones of the Pin Dale-Bradwell Moor area of Derbyshire. Compte Rendu, 6th Congress International Stratigraphie et Geologie Carbonifere No 3, pp 1249–1262
Parkinson D (1952) Allometric growth in *Dielasma hastata* from Treak Cliff, Derbyshire. Geol J 89:201–216. https://doi.org/10.1017/S0016756800067613
Payne JL, Heim NA, Knope ML, McClain CR (2014) Metabolic dominance of bivalves predates brachiopod diversity decline by more than 150 million years. Proc R Soc B 28:20133122. https://doi.org/10.1098/rspb.2013.3122
Pérez-Huerta A, Sheldon ND (2006) Pennsylvanian sea level cycles, nutrient availability and brachiopod palaeoecology. Palaeogeogr Palaeoclimatol Palaeoecol 230:264–279. https://doi.org/10.1016/j.palaeo.2005.07.020
Phillips J (1836) Illustrations of the geology of Yorkshire. Part II. The Mountain Limestone District. John Murray, London
Pickard NAH (1992) Depositional controls on Lower Carboniferous microbial buildups, eastern Midland Valley of Scotland. Sedimentology 39:1081–1100. https://doi.org/10.1111/j.1365-3091.1992.tb01998.x
Pickard NAH (1996) Evidence for microbial influence on the development of Lower Carboniferous buildups. In: Strongen P, Somerville ID, Jones GLL (eds) Recent advances in Lower Carboniferous Geology. Geol Soc Spec Publ No 107, pp 65–82. https://doi.org/10.1144/GSL.SP.1996.107.01.06
Piper JDA, Atkinson D, Norris S, Thomas S (1991) Palaeomagnetic study of the Derbyshire lavas and intrusions, Central England: definition of Carboniferous apparent polar wander. Phys Earth Planet Int 69:37–55. https://doi.org/10.1016/0031-9201(91)90152-8
Poty E, Aretz M, Barchy L (2002) Stratigraphie et sédimentologie des « Calcaires à *Productus* » du Carbonifère inférieur de la Montagne noire (Massif central, France). Comp Rend Acad Sc Paris Géosc 334:843–848. https://doi.org/10.1016/S1631-0713(02)01818-7
Pratt BR (1995) The origin, biota and evolution of deep-water mud mounds. In: Monty CLV, Bosence DWJ, Bridges PH, Pratt BR (eds) Carbonate mud mounds: their origin and evolution. IAS Sp Publ No 23, pp 49–123. https://doi.org/10.1002/9781444304114.ch3
Pray LC (1958) Fenestrate bryozoan core facies, Mississippian bioherms, southwestern United States. J Sediment Petrol 28:261–273. https://doi.org/10.1306/74D707D1-2B21-11D7-8648000102C1865D
Precht WF, Shepard W (1989) The structure, sedimentology and diagenesis of some Waulsortian carbonate buildups of Mississippian age from Montana. In: Geldsetzer HHJ, James NP, Tebbutt GE (eds) Reefs, Canada and Adjacent Areas. Mem Can Soc Petrol Geol No 13, pp 682–687
Ramsbottom WHC (1973) Transgressions and regressions in the Dinantian: a new synthesis of British Dinantian stratigraphy. Proc York Geol Soc 39:567–607. https://doi.org/10.1144/pygs.39.4.56
Ramsbottom WHC (1977) Major cycles of transgression and regression (mesothems) in the Namurian. Proc York Geol Soc 41:261–291. https://doi.org/10.1144/pygs.41.3.261
Rauzer-Chernousova DM, Fursenko AV (1937) Determination of foraminifera in the oil bearing regions of the USSR, pt.1. Leningrad, Moscow. [in Russian]
Reitner J (1993) Modern cryptic microbialite/metazoan facies from Lizard Island (Great Barrier Reef, Australia) formation and concepts. Facies 29:3–39. https://doi.org/10.1007/BF02536915
Reitner J, Neuweiler F (1995) Mud mounds: recognizing a polygenetic spectrum of fine-grained carbonate buildups. In: Reitner J, Neuweiler F (eds) A polygenetic spectrum of fine-grained carbonate buildups. Facies 32:2–4
Reitner J, Gautret P, Marin F, Neuweiler F (1995a) Automicrites in a modern marine microbialite. Formation model via organic matrices (Lizard Island, Great Barrier Reef, Australia). Bull Inst Océan Monaco Spec Issue No 14, pp 237–263
Reitner J, Neuweiler F, Gautret P (1995b) Modern and fossil automicrites: implications for mud mound genesis. In: Reitner J, Neuweiler F (eds) A polygenetic spectrum of fine-grained carbonate buildups. Facies 32:4–17
Riding R (2000) Microbial carbonates: the geological record ofn calcified bacterial-algal mats and biofilms. Sedimentology 47:179–214. https://doi.org/10.1046/j.1365-3091.2000.00003.x
Riding R (2002) Structure and composition of organic reefs and carbonate mud mounds: concepts and categories. Earth Sc Rev 58:163–231. https://doi.org/10.1016/S0012-8252(01)00089-7
Ross CA, Ross JR (1985) Late Paleozoic depositional sequences are synchronous and worldwide. Geology 13:194–197. https://doi.org/10.1130/0091-7613(1985)13%3c194:LPDSAS%3e2.0.CO;2
Rygel MC, Fielding CR, Frank TD, Birgenheier LP (2008) The magnitude of Late Paleozoic glacioeustatic fluctuations: a synthesis. J Sed Res 78:500–511. https://doi.org/10.2110/jsr.2008.058
Schwarzacher W (1961) Petrology and Structure of Some Lower Carboniferous Reefs in Northwestern Ireland. Bull Am Ass Petrol

Geol 46:1481–1503. https://doi.org/10.1306/BC7436FB-16BE-11D7-8645000102C1865D
Sevastopulo GD (1982) The age and depositional setting of Waulsortian limestones in Ireland. In: Bolton K, Lane HR, LeMone DV (eds) Symposium on the environmental setting and distribution of the Waulsortian facies. El Paso Geol Soc and Univ Texas, El Paso, pp 65–79
Sevastopulo GD, Barham M (2014) Correlation of the base of the Serpukhovian Stage (Mississippian) in NW Europe. Geol Mag 151:244–253. https://doi.org/10.1017/S0016756813000630
Shen Y, Neuweiler F (2018) Questioning the microbial origin of automicrite in Ordovician calathid–demosponge carbonate mounds. Sedimentology 65:303–333. https://doi.org/10.1111/sed.12394
Shen JW, Webb GE (2005) Metazoan–microbial fabrics in a Mississippian (Carboniferous) coral–sponge–microbial reef, Monto, Queensland, Australia. Sediment Geol 178:113–133. https://doi.org/10.1016/j.sedgeo.2005.03.011
Shen JW, Webb GE (2008) The role of microbes in reef-building communities of the Cannindah limestone (Mississippian), Monto region, Queensland, Australia. Facies 54:89–105. https://doi.org/10.1007/s10347-007-0116-2
Shiells KAG, Penn IE (1971) Notes on the geology of Trearne Quarry (Upper Visean), Ayrshire and on the palaeoecology of its productid brachiopods. Scott J Geol 7:29–49. https://doi.org/10.1144/sjg07010029
Smith Jr LB, Read JF (2000) Rapid onset of late Paleozoic glaciation on Gondwana: evidence from Upper Mississippian strata of the Midcontinent, United States. Geology 28:279–282. https://doi.org/10.1130/0091-7613(2000)28%3c279:ROOLPG%3e2.0.CO;2
Smith K, Smith NJP, Holliday DW (1985) The deep structure of Derbyshire. Geol J 20:215–225. https://doi.org/10.1002/gj.3350200303
Smith R, Martill DM, Duffin C (2017) The shark-beds of the Eyam Limestone Formation (Lower Carboniferous, Viséan) of Steeplehouse Quarry, Wirksworth, Derbyshire, UK. Proc Geol Ass 128:374–400. https://doi.org/10.1016/j.pgeola.2017.04.004
Smith EG, Rhys GH, Eden RA, Calver MA, Duff PMD, Harrison RK, Ramsbottom WHC (1967) Geology of the country around Chesterfield, Matlock and Mansfield. Explanation of sheet 112. British Geological Survey, Keyworth, Nottingham, p. vii + 430
Somerville ID (2003) Review of Irish Lower Carboniferous (Mississippian) mud mounds: depositional setting, biota, facies, and evolution. In: Ahr WM, Harris PMM, Morgan WA, Somerville ID (eds) Permo-Carboniferous carbonate platforms and reefs. SEPM Spec Publ No 78, AAPG Memoir No 83, pp 239–252. https://doi.org/10.2110/pec.03.78.0239
Somerville ID, Strogen P, Jones GL (1992) Mid-Dinantian Waulsortian buildups in the Dublin Basin, Ireland. Sediment Geol 79:91–116. https://doi.org/10.1016/0037-0738(92)90006-D
Somerville ID, Cózar P, Aretz M, Herbig HG, Mitchell WI, Medina-Varea P (2009) Carbonate facies and biostromal distribution in a tectonically controlled platform in northwestern Ireland during the late Viséan (Mississippian). Proc York Soc Geol 57:165–192. https://doi.org/10.1144/pygs.57.3-4.165
Sowerby J (1812–1815) The Mineral Conchology of Great Britain, vol 1. Published by the author, London, p 234. https://doi.org/10.5962/bhl.title.14408
Sowerby J (1821–1822) The Mineral Conchology of Great Britain,vol 4. Published by the author, London, p 114. https://doi.org/10.5962/bhl.title.14408
Sowerby J de C (1823–1825) The Mineral Conchology of Great Britain, vol 5. Published by the author, London, p 168. https://doi.org/10.5962/bhl.title.14408
Stevenson IP, Gaunt GD (1971) Geology of the country around Chapel−en−Frith. Memoir of the British Geological Survey. Sheet 99. British Geological Survey, Keyworth, Nottingham, p. xii + 444
Stone P, Millward D, Young B, Merritt JW, Clark SM, McCormac M, Lawrence DJD (2010) British regional geology: Northern England, Fifth ed. British Geological Survey, Nottingham, p. ix + 294
Tiddemann RH (1889) On concurrent faulting and deposition in Carboniferous times in Craven, Yorkshire, with a note on Carboniferous reefs. Rep Br Assoc Adv Sci 2:600–603
Timms AE (1978) Aspects of the palaeoecology of productoid and associated brachiopods in the middle to upper Visean 'reef' limestones of Derbyshire. PhD thesis, University of Manchester, Manchester, p. x+344
Tout J, Astudillo-García C, Taylor MW, Tyson GW, Stocker R, Ralph PJ, Seymour JR, Webster NS (2017) Redefining the sponge-symbiont acquisition paradigm: sponge microbes exhibit chemotaxis towards host-derived compounds. Environ Microbiol Rep 9:750–755. https://doi.org/10.1111/1758-2229.12591
Trichet J, Défarge C (1995) Non-biologically supported organomineralization. Bull Inst océan Monaco Spec Issue, pp 203–236
Tsien HH (1985) Origin of stromatactis-a replacement of colonial microbial accretions. In: Toomey DF, Nitecki MH (eds) Paleoalgology: contemporary research and applications. Springer-Verlag, Berlin, pp 274–289
Vacelet J, Donadey C (1977) Electron microscope study of the association between some sponges and bacteria. Jour Exp Mar Biol Ecol 30:301–314. https://doi.org/10.1016/0022-0981(77)90038-7
Vachard D, Cózar P, Aretz M, Izart A (2016) Late Viséan-Serpukhovian foraminifers in the Montagne Noire (France): Biostratigraphic revision and correlation with the Russian substages. Geobios 49:469–498. https://doi.org/10.1016/j.geobios.2016.09.002
Vachard D, Izart A, Cózar P (2017) Mississippian (middle Tournaisian-late Serpukhovian) lithostratigraphic and tectonosedimentary units of the southeastern Montagne Noire (Hérault, France). Géol Fr 1:47–88
von Bitter PH, Scott SD, Schenk PE (1990) Early Carboniferous low-temperature hydrothermal vent communities from Newfoundland. Nature 344:145–148. https://doi.org/10.1038/344145a0
von Bitter PH, Scott SD, Schenk PE (1992) Chemosynthesis: an alternate hypothesis for Carboniferous biotas in bryozoan/microbial mounds, Newfoundland, Canada. Palaios 7:466–484. https://doi.org/10.2307/3514830
Walkden GM (1987) Sedimentary and diagenetic styles in late Dinantian carbonates of Britain. In: Miller J, Adams AE, Wright QP (eds) European Dinantian environments. Wiley, Chichester, pp 131–155
Warnke K (1995) Calcification processes of siliceous sponges in Viséan limestones (counties Sligo and Leitrim, Northwestern Ireland). Facies 33:215–227. https://doi.org/10.1007/BF02537453
Waters CN, Waters RA, Barclay WJ, Davies JR (2009) A lithostratigraphical framework for the Carboniferous successions of southern Great Britain (Onshore). British Geological Survey Research Report RR/09/01, p. 184
Waters CN, Somerville ID, Jones NS, Cleal CJ, Collinson JD, Waters RA, Besly BM, Dean MT, Stephenson MH, Davies JR, Freshney EC, Jackson DI, Mitchell WI, Powell JH, Barclay WJ, Browne MAE, Leveridge BE, Long SL, McLean D (2011) A revised correlation of Carboniferous rocks in the British Isles. Geol Soc London Sp Report, No 26, p 186
Waters CN, Haslam RB, Cózar P, Somerville ID, Millward D, Woods M (2017) Mississippian reef development in the Cracoe Limestone Formation of the southern Askrigg Block, North Yorkshire, UK. Proc York Geol Soc 61:179–196. https://doi.org/10.1144/pygs2016-374
Webb GE (1987) Late Mississippian thrombolite bioherms from the Pitkin Formation of northern Arkansas. Geol Soc Am Bull

99:686–698. https://doi.org/10.1130/0016-7606(1987)99%3c686:LMTBFT%3e2.0.CO;2
Webb GE (1996) Was Phanerozoic reef history controlled by the distribution of non-enzymatically secreted reef carbonates (microbial carbonate and biologically induced cement)? Sedimentology 43:947–971. https://doi.org/10.1111/j.1365-3091.1996.tb01513.x
Webb GE (1999) Youngest Early Carboniferous (Late Visean) Shallow-Water Patch Reefs in Eastern Australia (Rockhampton Group, Queensland): Combining Quantitative Micro- and Macro-Scale Data. Facies 41:111–140. https://doi.org/10.1007/BF02537462
Webb GE (2001) Biologically induced carbonate precipitation in reefs through time. In: Stanley GD (ed.) The history and sedimentology of ancient reef systems. Kluwer Academic Publishers, New York, pp 159–203. https://doi.org/10.1007/978-1-4615-1219-6_5
Webb GE (2002) Latest Devonian and Early Carboniferous reefs: depressed reef building after the middle Paleozoic collapse. In: Kiessling W, Flügel E, Golonka J (eds) Phanerozoic reef patterns. SEPM Special Publications No 72, pp 239–269. https://doi.org/10.2110/pec.02.72.0239
Weiner S, Dove PM (2003) An overview of biomineralization and the problem of the vital effect. In: Dove PM, Weiner S, De Yoreo JJ (eds) Biomineralization. Mineralogical Society of America. Review in Mineralogy and Geochemistry, vol 54. Washington, D.C., pp 1–31
Wendt J, Kaufmann B, Belka Z (2001) An exhumed Palaeozoic underwater scenery: the Visean mud mounds of the eastern anti-Atlas (Morocco). Sediment Geol 145:215–233. https://doi.org/10.1016/S0037-0738(01)00149-X
Wilkinson CR (1978a) Microbial associations in sponges I. Ecology, physiology and microbial populations of coral reef sponges. Mar Biol 49:161–167. https://doi.org/10.1007/BF00387115
Wilkinson CR (1978b) Microbial associations in sponges II. Numerical analysis of sponge and water bacterial populations. Mar Biol 49:169–176. https://doi.org/10.1007/BF00387116
Wilkinson CR, Garrone R, Vacelet J (1984) Marine sponges discriminate between food bacteria and bacterial symbionts: electron microscope radioautography and in-situ evidence. Proc R Soc Lond B 220:519–528. https://doi.org/10.1098/rspb.1984.0018
Wilkinson CR, Trott LA (1985) Light as a factor determining the distribution of sponges across the central Great Barrier Reef. In: Proc Fifth Int Coral Reef Congr Tahiti, pp 125–130
Wilson JL (1974) Characteristics of carbonate platform margins. Bull Am Ass Petrol Geol 58:810–824
Wolf KH (1965) Gradational sedimentary products of calcareous algae. Sedimentology 5:1–37. https://doi.org/10.1306/83D9149D-16C7-11D7-8645000102C1865D
Wolfenden EB (1958) Paleoecology of the Carboniferous reef complex and shelf limestones in Northwest Derbyshire, England. Bull Geol Soc Am 60:871–898. https://doi.org/10.1130/0016-7606(1958)69[871:POTCRC]2.0.CO;2
Woods CHC, Lee JR (2018) The geology of England: critical examples of Earth history—an overview. Proc Geol Ass 129:255–263. https://doi.org/10.1016/j.pgeola.2018.01.007
Wright VP, Faulkner TJ (1990) Sediment dynamics of early carboniferous ramps: A proposal. Geol J 25:139–144. https://doi.org/10.1002/gj.3350250205
Wright VP, Vanstone SD (2001) Onset of Late Palaeozoic glacio-eustasy and the evolving climates of low latitude areas: a synthesis of current understanding. J Geol Soc 158:579–582. https://doi.org/10.1144/jgs.158.4.579
Yao L, Aretz M (2020) Upper Visean (Mississippian) metazoan microbial reefs from Guangxi, South China: Insights regarding reef recovery after the end-Devonian extinction. Palaeogeogr Palaeoclimatol Palaeoecol 560:109994. https://doi.org/10.1016/j.palaeo.2020.109994
Yao L, Aretz M, Chen JT, Webb E, Wang X (2016) Global microbial carbonate proliferation after the end-Devonian mass extinction: Mainly controlled by demise of skeletal bioconstructors. Sci Rep 6:39694. https://doi.org/10.1038/srep39694
Yao L, Aretz M, Wignall PB, Chen J, Vachard D, Qi Y, Shen S, Wang X (2020) The longest delay: re-emergence of coral reef ecosystems after the Late Devonian extinctions. Earth Sc Rev 203:103060. https://doi.org/10.1016/j.earscirev.2019.103060
Zhou K, Pratt BR (2019) Composition and origin of stromatactis-bearing mud mounds (Upper Devonian, Frasnian), southern Rocky Mountains, western Canada. Sedimentology 66:2455–2489. https://doi.org/10.1111/sed.12595